

UNCLASSIFIED

AD NUMBER

AD826369

LIMITATION CHANGES

TO:

Approved for public release; distribution is unlimited. Document partially illegible.

FROM:

Distribution authorized to U.S. Gov't. agencies and their contractors;
Administrative/Operational Use; 1956. Other requests shall be referred to United States Naval Postgraduate School, Monterey, CA 93943.
Document partially illegible.

AUTHORITY

USNPS ltr dtd 6 Oct 1971

THIS PAGE IS UNCLASSIFIED

LOAN DOCUMENT

**STEADY AND OSCILLATORY FLOW FORCES
ON A MARK 6 MOORED MINE**

James Patrick McMahon

AD- 826369

releas



Library
USS Naval Postgraduate School
Monterey, California

STEADY AND OSCILLATORY FLOW FORCES
ON A MARK 6 MOORED MINE

by

James Patrick McMahon
Lieutenant, United States Navy

Submitted in partial fulfillment
of the requirements
for the degree of
MASTER OF SCIENCE

AD-826,369

United States Naval Postgraduate School
Monterey, California

1956

This work is accepted as fulfilling
the thesis requirements for the degree of

MASTER OF SCIENCE

from the
United States Naval Postgraduate School

Approved:



PREFACE

The work on this thesis was accomplished during the period January to May, 1956, at the United States Naval Postgraduate School, Monterey, California.

The author wishes to express his appreciation for the advice and encouragement of Professor J. B. Wickham under whose direction this study was carried out. The advice and suggestions of Professors W. C. Thompson and W. E. Bleick are gratefully acknowledged.

The writer is also greatly indebted to Mrs. Jane Whitney for her excellent job in preparing this manuscript.

TABLE OF CONTENTS

Item	Title	Page
Certificate of Approval		i
Preface		ii
Table of Contents		iii
Abstract		iv
List of Figures and Tables		v
Table of Notation		vii
Chapter 1	Introduction	1
Chapter 2	Steady Flow Forces	3
Chapter 3	Oscillatory Flow Forces	27
Chapter 4	Conclusions	58
Bibliography		60
Appendix A	Chain Characteristics	62
Appendix B	Wire Rope Engineering Data	63
Appendix C	Forces on a Moored Mine Due to Uniform Fluid Flow	66
Appendix D	Overturning Movement on a Mark 6 Anchor	81
Appendix E	Natural Heaving Period of a Mark 6 Mine	83
Appendix F	Natural Surging Period of a Mark 6 Mine	84
Appendix G	Maximum Horizontal Wave Force Exerted on Mine Cables in Shallow Water	85
Appendix H	Maximum Vertical Force Exerted on a Mine Case	87

ABSTRACT

A theoretical investigation is made of the forces acting upon a moored mine due to uniform and oscillatory fluid flow. The general problem is discussed analytically and approximate methods are presented to ascertain the forces to be expected.

LIST OF FIGURES AND TABLES

Figure		Page
1	Effective Roughness - Influence of Concentration	9
2	Drag Coefficients for various bodies	12
3	Drag Coefficients for Spheres with varying degrees of Surface Roughness	13
4	Karman Vortex Street	14
5	Drag Coefficient vs Amplitude of an Oscillatory Cylinder	16
6	Simplified Diagram of the Forces acting on a Moored Mine	20
7	Wave Nomenclature	28
8	Trajectories and Streamlines of Particle Motion in a Progressive Wave	29a
9	Illustrations of various functions of K_h	35a
10	Coordinate system	40
11	Idealized scheme of moored mine with a fictitious spring representing the effective spring constant of the wire rope cable	41
12	Mine case displaced a small distance ϵ from its equilibrium position	44a
13	Forces on a Cable Segment due to Wave Motion	48
14	General Relation of Surface to Sub-Surface Tidal Current	67
15	Forces on a Cable Segment	69
16	Differential Triangle	71
17	Free body diagram of a Cable Segment	71
18	Forces on a Moored Mine and Cable	72a
19	Cable Segment	73
20	External Forces acting on a Mark 6 Anchor	81

Table		Page
I	Mine Dip and Forces exerted on a Mark 6 Mine moored with various cable lengths in a steady three knot current	22
II	Behavior of Mark 6 type anchor in different type bottoms	26
III	Orbital diameter and particle velocity as a function of depth	32
IV	Approximate Natural Heaving Period of Mark 6 type Mine	43
V	Approximate Natural Surging Periods of Mark 6 Type Mines vs cable length	46
VI	Maximum Vertical Force exerted on a Mark 6 Mine Case moored 20 feet below the sea surface in Deep Water	56
VII	Maximum Vertical Force exerted on a Mark 6 Mine Case moored ten feet below the sea surface in a depth of 50 feet (Intermediate depth)	57
VIII	Maximum Vertical Force exerted on a Mark 6 Mine Case moored 20 feet below the sea surface in a depth of 50 feet (Intermediate depth)	57
IX	Weight and Size Characteristics of Uncoated or Galvanized Steel Proof Coil Chains	62
X	Wire Rope Characteristics	64
XI	Comparison of Dip Values obtained using various section combinations	78
XII	The Deep Water Wave Lengths and Periods of Shallow Water Waves in certain depths	85

Table		Page
I	Mine Dip and Forces exerted on a Mark 6 Mine moored with various cable lengths in a steady three knot current	22
II	Behavior of Mark 6 type anchor in different type bottoms	26
III	Orbital diameter and particle velocity as a function of depth	32
IV	Approximate Natural Heaving Period of Mark 6 type Mine	43
V	Approximate Natural Surging Periods of Mark 6 Type Mines vs cable length	46
VI	Maximum Vertical Force exerted on a Mark 6 Mine Case moored 20 feet below the sea surface in Deep Water	56
VII	Maximum Vertical Force exerted on a Mark 6 Mine Case moored ten feet below the sea surface in a depth of 50 feet (Intermediate depth)	57
VIII	Maximum Vertical Force exerted on a Mark 6 Mine Case moored 20 feet below the sea surface in a depth of 50 feet (Intermediate depth)	57
IX	Weight and Size Characteristics of Uncoated or Galvanized Steel Proof Coil Chains	62
X	Wire Rope Characteristics	64
XI	Comparison of Dip Values obtained using various section combinations	78
XII	The Deep Water Wave Lengths and Periods of Shallow Water Waves in certain depths	85

TABLE OF NOTATION

The following is a list of the symbols used in this paper.

Symbol	Definition	Unit
A	Area	feet ²
A _M	Area of the projection of a mine case on a plane normal to the direction of fluid flow	feet ²
A _W	Metallic area of wire rope cross section	in. ²
B	Positive buoyancy of mine case	lbs
C	Wave velocity	ft/sec.
C _D	Coefficient of drag	--
C _f ¹	Average tangential drag coefficient for chain	--
C _f	Average skin friction drag coefficient	--
C _i	Individual sections of cable or chain are denoted C ₁ , C ₂C _n . C _i is any cable section selected for analysis; i is equal to any number from 1 to n.	--
C _M	Coefficient of mass	--
C _o	Deep water wave velocity	ft/sec.
C _p	Coefficient of pressure drag	--
C _s	Shallow water wave velocity	ft/sec.
D	Drag	lbs
D _f	Tangential or skin friction drag	lbs
D _p	Pressure drag	lbs
D _T	Total drag	lbs

d	Cable diameter	ft
d_1	Diameter of cable section C_1	ft
d_L	Overall width of chain link	ft
d_M	Diameter of mine case	ft
d_T	Actual diameter of bar stock from which a chain is manufactured	in.
E	Modulus of Elasticity	lbs/in. ²
F	Any force	lbs
F_A	Force transmitted to the anchor by the mine cable	lbs
F_{HT}	Total horizontal component of the oscillatory force exerted on a mine cable	lbs
$\overline{F_{HT}}$	Maximum total horizontal component of the oscillatory force exerted on a mine cable	lbs
F_1	Drag force on the cable section C_1 when the cable is normal to the flow	lbs
F_{VT}	Total vertical component of the oscillatory force exerted on a mine case	lbs
$\overline{F_{VT}}$	Maximum total vertical component of the oscillatory force exerted on a mine case	lbs
f	The drag per foot of an arbitrary cable when the cable is normal to the flow	lbs/ft
f'	The tangential drag per foot of chain	lbs/ft
f_1	The drag per foot of the cable section C_1 when the cable is normal to the flow	lbs/ft
f_r	Frequency	cycles/sec.
f_T	The drag per foot parallel to the cable axis	lbs/ft

G_1	The value of $\tan \beta_1$	- -
g	Acceleration of gravity	ft/sec ²
H	Wave height	feet
h	Depth of water measured from the undisturbed water level to the bottom	feet
K	Wave number $\frac{2\pi}{L}$	$\frac{1}{\text{feet}}$
k	Height of sand for equivalent sand roughness	feet
L	Wave length	feet
L_o	Deep water wave length	feet
L_s	Shallow water wave length	feet
l, ℓ	A linear dimension	feet
l_1, l_i	The length of cable section C_1	feet
M	Any mass	slugs
M'	Mass of fluid displaced by an arbitrary object	slugs
M_c	Mass of a mine cable which acts as part of the oscillatory mass in an oscillating mine	slugs
M_g	Effective mass of an oscillating mine case and cable	slugs
N	Overturning moment	ft/lbs
N_R	Reynold's Number = $\frac{lU}{\nu}$ where l is the governing linear dimension in the flow pattern, e.g., the diameter of a mine case. U is the velocity of the fluid relative to a body and ν is the kinematic viscosity.	- -
N_S	Strouhal's Number = $\frac{f_r d}{U}$ where f_r is the frequency in cycles/sec., d is the diameter of a circular cylinder, or the significant linear dimension of a noncircular cylinder, U is the velocity of the fluid relative to a body	- -

n	The total number of cable sections in a mooring	--
q	Inertial coefficient	--
R	Any force	lbs
R_H	Any horizontal force	lbs
R_V	Any vertical force	lbs
s	The length of the mine cable from the mine case to the anchor	feet
S_u	Area of surface tangent to flow	feet ²
S	Elastic stretch of a wire rope mine cable	feet
T	Wave period	sec.
T_e	Tensile load in a cable at an arbitrary point	lbs
t	A time	sec.
U	Uniform current velocity	ft/sec.
u	Horizontal component of water particle orbital velocity	ft/sec.
V	Any volume	feet ³
W	Any weight	lbs
W_A	Weight in sea water of mine anchor	lbs
W_1	Weight in sea water of the cable section C_1	lbs
W_M	Weight of mine case in air	lbs
w	Vertical component of water particle orbital velocity	ft/sec.
w	Weight per foot in sea water of any cable	lb/ft
w_1	Weight per foot in sea water of the cable section C_1	lb/ft
w'	Weight per foot in air of any cable	lb/ft

X	Any extraneous force in the x direction	lbs
X_A	The horizontal component of the force transmitted to the anchor by the mine cable	lbs
X_1	The horizontal component of the tension at the upper end of the cable section C_1	lbs
X_1'	The horizontal component of the tension at the lower end of the cable section C_1	lbs
x	A horizontal distance from an arbitrary origin	feet
Y	Any extraneous force in the y direction	lbs
Y_A	The vertical component of the force transmitted to the anchor by the mine cable	lbs
Y_1	The vertical component of the tension at the upper end of the cable section C_1	lbs
Y_1'	The vertical component of the tension at the lower end of the cable section C_1	lbs
y	A distance from an arbitrary origin	feet
Z, z	A vertical distance from an arbitrary horizontal plane	feet
α (alpha)	Any angle	degrees
α_1	The angle between the cable section C_1 and the vertical	degrees
β_1 (beta)	First estimate of the angle between the cable section C_1 and the vertical	degrees
γ_1 (gamma)	Second estimate of the angle between the cable section C_1 and the vertical	degrees
Δ (delta)	A change	as stated
δ (delta)	Mine case dip	feet
ϵ (epsilon)	A small linear displacement	feet

ϵ_H (epsilon H)	A small linear displacement in the horizontal direction	feet
ϵ_V (epsilon V)	A small linear displacement in the vertical direction	feet
ζ (zeta)	Vertical displacement of water particle from equilibrium position	feet
η (eta)	Wave surface elevation above undisturbed level	feet
θ (theta)	Angular position of a water particle in its orbit = $Kx - \sigma t$	--
λ (lambda)	Ratio $\frac{\sinh K(h+z)}{\sinh Kh}$	--
μ (mu)	Coefficient of friction	--
μ_{crit}	Critical value of the coefficient of friction	--
ν (nu)	Kinematic viscosity	ft ² /sec.
ξ (xi)	Horizontal displacement of water particle from equilibrium position	feet
π (pi)	3.1416	--
ρ (rho)	Mass density of sea water	slugs/ft ³
σ (sigma)	Angular velocity = $\frac{2\pi}{T}$	radians/sec.
ϕ (phi)	That value of θ where the vertical component of the oscillatory force on a mine case is at a maximum	--

ABBREVIATIONS

The following abbreviations have been used:

DTMB	David W. Taylor Model Basin
NACA	National Advisory Committee for Aeronautics
NOL	Naval Ordnance Laboratory
NOLM	Naval Ordnance Laboratory Memorandum
NOLR	Naval Ordnance Laboratory Report
cps	cycles per second
u.w.l.	undisturbed water level

CHAPTER 1

INTRODUCTION

The effectiveness of moored contact mines is dependent to a large extent upon the ocean environment. The object in this paper has been to examine a limited segment of this environment, namely fluid flow, in an attempt to determine its influence on moored contact mine effectiveness.

The problem to be considered can be exemplified by the following situation.

If a positively buoyant mine is planted in still water the mine case assumes a position directly over the anchor at a height above the bottom equal to the length of the mooring cable. In the presence of fluid flow the same mine case will be displaced both vertically and horizontally due to the hydrodynamic forces on the mine case and cable. If these forces are very strong the entire mine assemblage may slide or "walk" along the bottom. The term "walking" refers to the situation where the mine anchor is lifted clear of the bottom; the entire mine assemblage then jumps or skips along the bottom in the direction of the prevailing current.

The vertical displacement of the mine case from its position in still water is usually called "dip". If the steady current forces are of sufficient magnitude the mine case may be deeper than the draft of ships it is intended to destroy. Thus, the mine may be rendered impotent if contact is required for actuation.

Movement of a moored mine is undesirable for a number of reasons. Among them are:

1. Mine may move into channels or areas frequented by friendly ships.

2. Mine may move into shallower water becoming exposed to visual detection.

3. Mine may move into deeper water, hence rendered impotent if contact is required for actuation.

Hydrodynamic forces also act in a third way to lessen the effectiveness of moored mines. The continual flexing and bending of the wire rope cables commonly used causes fatigue and eventual breaking of the cable.

In attempting to predict the behavior of a mine moored in the ocean a twofold problem arises; fluid forces due to tide and wind-induced currents, which may be considered as steady, and oscillatory fluid forces due to wind generated waves.¹ While the steady fluid forces on a moored mine have been treated hitherto² the possible effects of marine fouling in changing the hydrodynamic characteristics of a spherical mine case or cylindrical cable were not considered. A semi-quantitative argument is presented herein to show that marine fouling increases the fluid forces primarily by increasing the size of the mine case and cable. Insofar as known no previous attempt has been made to predict the forces on a moored mine due to wave motion.

The problem has been simplified by assuming steady and oscillatory flow and forces are independent of one another and that ocean waves have simple sinusoidal profiles. Mathematical expressions are then developed which permit the numerical computation of the forces involved. The appendices describe the methods used in arriving at numerical values presented.

1 Forces due to eddies or swirls and various long-period gravity waves will not be considered herein.

2 The most complete general treatment insofar as is known to the author is contained in NOLR 380.

CHAPTER 2

STEADY FLOW FORCES

The objective of this chapter is to examine the forces exerted on a moored mine assemblage by uniform fluid flow.

2A FLUID MOTION

When an object is immersed in a uniform fluid flow the resultant force on the body can be divided into two components, lift and drag. Lift is defined as the force in the direction normal to that of fluid flow and drag is the force whose direction coincides with that of the fluid. Since we will be dealing with steady flow in a horizontal direction lift and drag act vertically and horizontally, respectively.

In this paper primary emphasis will be placed on the drag force which can be further subdivided as follows:

Tangential Force - The shear forces at the surface of the body due to the frictional effects in the boundary layer.¹ This force may be represented by

$$D_f = \frac{1}{2} C_f \int S_u U^2$$

Normal Force - The pressure force resulting from the variation in pressure over the surface of the body. This force may be represented by

$$D_p = \frac{1}{2} C_p \int A U^2$$

1 See page 5, infra.

Usually the total drag force is expressed in terms of a single equation

$$D_T = \frac{1}{2} C_D \int AU^2$$

2A1 LAMINAR FLOW

In laminar flow the fluid particles moving as units are of molecular size and move in parallel layers of infinitesimal thickness. These layers slide over adjacent layers but do not intermingle or mix except on a molecular scale. In this sliding motion there exists internal friction if the adjacent layers are in motion relative to one another. This enables moving liquid particles to drag along adjacent particles previously at rest and accounts for the skin friction or frictional drag force in laminar boundary flow [1] .

2A2 TURBULENT FLOW

Turbulent flow differs from laminar in that much larger masses of fluid move together as units. This movement occurs in a haphazard and chaotic fashion with the units continually breaking down and intermingling. The flow is one of random motion usually superimposed on a steady flow such as an ocean current or atmospheric wind. Periodic wave motion or the movement of large bodies of fluid, which can be attributed to a source of disturbance such as tides or wind, are not classed as turbulent flow even though they do vary with time. Here, the essential element of randomness is missing, i.e., there is a discernible pattern. It must be pointed out, however, that once fluid motion is started in the ocean, the environment is such that the development of turbulent flow is favored. This is further discussed by Sverdrup, et.al., [2] and Kuenen [3] .

In laminar flow frictional drag was attributed to internal friction or viscous action resulting in an exchange of momentum. This process is of much greater importance in turbulent flow since momentum exchange is increased by the vigorous mixing action. This leads to an increased frictional drag.

2A3 BOUNDARY LAYER

When an obstruction is placed in a fluid stream a very thin film of fluid in contact with its surface is brought to rest while fluid at some distance away from the surface maintains the original free stream velocity. The transition layer where the velocity is changing due to the obstruction is termed the boundary layer. Boundary layers exist because of momentum exchanges and are classified as laminar or turbulent depending on the extent of this exchange. The classification of the boundary layer is independent of the type of free stream flow. It is possible to have a laminar boundary in a turbulent-free stream and vice versa.

The following factors favor the development of a turbulent boundary layer [4] :

1. Free stream turbulence
2. Acoustic noise
3. Surface roughness
4. Positive pressure gradient
5. High Reynolds Numbers

The first two factors are almost always present in ocean flow. In addition, the method of mooring a mine adds to the noise and turbulence due to oscillation of the mine case and cable.

In considering surface roughness, even though we assume a mine case is hydrodynamically smooth at the time of planting,² the slime film which forms even on surfaces coated with anti-fouling paint [5] would produce a hydrodynamically rough surface in a few days. Further, a mine case is normally fitted with padeyes, horns, welded seams, access fittings, etc., all tending to cause the boundary layer to turn turbulent prematurely. Mine mooring cables are either stranded wire or chain and also would be classed as rough surfaces.

A positive pressure gradient, where pressure increases in the direction of fluid motion, exists on a smooth sphere from the diametral plane aft. Since the fluid adjacent to the surface in this region is proceeding into an area of increasing pressure it is retarded. Fluid particles farther from the surface are retarded to a lesser degree. The result is eddy formation and turbulence.

A negative pressure gradient, which favors a laminar boundary layer, exists from the nose to the diametral plane [4]. However, the surface of a spherical mine is liberally fitted with protuberances as mentioned heretofore. Each of these protuberances disturbs the flow resulting in a highly distorted, nonuniform velocity field and, therefore, a turbulent boundary layer.

A smooth circular cylinder with its axis normal to fluid flow has the same type of pressure gradient as a smooth sphere, i.e., negative from the nose to the point of maximum diameter, then positive. With a

2 See page 10, infra.

flexible vibrating mine cable moving in varying directions it can only be stated that the pressure gradient has no set pattern but is continuously changing with cable motion.

Increasing N_R eventually leads to a turbulent boundary layer even in the absence of all the above four conditions. For example, an upper limit of N_R of about 4×10^5 is indicated for a laminar boundary layer about a sphere [6]. At higher N_R transition from laminar to turbulent boundary flow occurs even on very smooth spheres in low turbulence mediums.

As a consequence of the above considerations only turbulent boundary layers will be considered in this paper.

2A4 HYDRODYNAMIC CLASSIFICATION OF BOUNDARY SURFACES

In order to discuss frictional effects in a semiquantitative manner certain descriptive terms used in Fluid Mechanics are introduced in this section and an attempt is made to classify mine surfaces according to their hydrodynamic properties.

2A4A LAMINAR SUB LAYER

Even when a turbulent boundary layer exists a thin layer immediately adjacent to the surface may be laminar in character. This is due to the presence of the boundary surface which prevents random motion of the fluid particles and channels the flow so as to follow the general surface contours. This very thin film is generally referred to as the laminar film or the laminar sub layer. The thickness of the laminar film varies inversely with N_R . For a given mine or cable this means that the higher the fluid velocity the thinner the laminar film.

2A4B DEFINITION OF HYDRODYNAMICALLY SMOOTH AND ROUGH SURFACES

A boundary surface is hydrodynamically smooth if the surface irregularities are so completely immersed in the laminar film that they do not influence the drag [4]. Conversely, a hydrodynamically rough surface is one in which surface irregularities contribute to a change in magnitude of the drag. Since the laminar film in water flows is usually only a small fraction of an inch thick it follows that a surface might be classified as rough even though the roughness elements were only a few thousandths of an inch in height. Further, because the laminar film becomes thinner with increasing N_R it is possible for the same surface to act as smooth or rough depending on N_R [1].

If the surface is extremely rough and many elements penetrate and disrupt the laminar film the resulting turbulence prevents the existence of a laminar film, according to Vennard [1].

2A4C EFFECTIVE ROUGHNESS

Since surface roughness can be described in many ways, height, shape, spacing, etc., of individual surface irregularities it has been found convenient to express surface roughness in terms of the grain diameter k of a uniform sand grain. In turn, k can be defined as the diameter of the sand grains which if attached in a tight concentration to a surface in lieu of the actual roughness elements would produce the same resistance to flow [4]. Effective roughness provides a basis for correlation of experimental data and permits the description of an irregular surface in terms of a single variable. Some authors use the term equivalent sand-grain roughness instead of effective roughness.

For a flat plate at zero incidence to flow the limiting k for a smooth surface is [4]

$$k = \frac{100 \nu}{U}$$

If we take $\nu = 1.28 \times 10^{-5}$ as an average value for sea water then for a current of one knot the limiting k for a smooth surface is about

$$k \leq 0.009 \text{ inches}$$

For a current of two knots

$$k \leq 0.005 \text{ inches}$$

While these values apply to flat plate over which no pressure gradient exists they do give an indication of the extreme smoothness required to produce a hydrodynamically smooth surface under ocean flow conditions.

Figure 1 shows the effective roughness of some common geometric shapes at different concentrations of roughness elements.

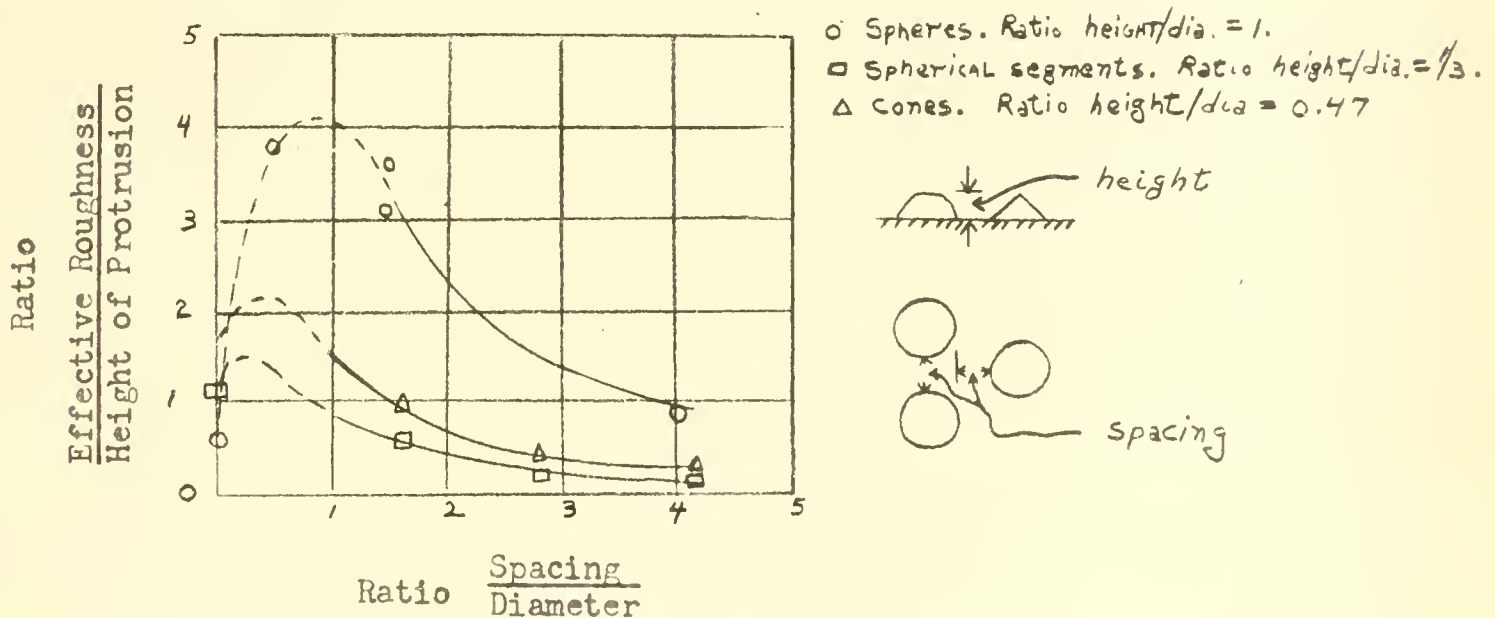


Figure 1 Effective roughness - Influence of Concentration (From S. Hoerner, Aerodynamic Drag [6])

It is seen that concentration or relative density is an important factor in determining k . A surface which is completely covered might actually have less drag than a surface on which the roughness elements are more sparse.

2A4D EFFECTIVE ROUGHNESS OF A MINE CASE

While no direct data on the effective roughness of a mine case is available the effective roughness for a newly launched ship is $k = 0.012$ inches, according to Schlichting [4]. The author believes that approximately the same value can be assumed for a steel sheet-metal mine case.

2A4E EFFECTIVE ROUGHNESS OF A PAINTED SURFACE

According to Young [7], the effective roughness of camouflage paints used on aircraft is approximately 0.001 to 0.01 inches. It is believed that paints used on mines must have larger values due to:

1. Greater thickness of the paint layer
2. Lack of effort to insure a ripple-free surface in painting mines in contrast with the great care taken in painting aircraft.

This is mentioned to point out that painting a surface does not necessarily produce a hydrodynamically smooth surface. Contrariwise, painting a hydrodynamically smooth surface may make it hydrodynamically rough.

2A4F EFFECTIVE ROUGHNESS OF MARINE GROWTHS

As far as known no data are available on the effective roughness of the various types of marine growth, although there are various cases cited in the literature on the relative increase in drag caused by marine growth. Schlichting [4], for example, mentions that the resistance of a ship can be increased fifty percent due to weeds adhering to the hull.

In the particular problem under study the lack of data on effective roughness of marine growth is not too serious as will be seen later.³

2B FLOW ABOUT A SMOOTH SPHERE OR CIRCULAR CYLINDER IN A LOW TURBULENCE MEDIUM

When N_R is low (about 10^3 to 10^5) the boundary layer is laminar.

As the fluid particles move over the forward or upstream section of the sphere boundary layer kinetic energy is consumed in overcoming friction forces. Due to this loss the boundary layer particles lack the energy to advance into the area of increasing pressure prevailing over the rear section, and the boundary layer separates from the surface just forward of the vertical diametral plane of the sphere. Because of the separation a large low pressure wake area containing irregular turbulent eddies forms on the downstream side of the sphere. The difference in pressure between the forward and downstream sections results in a force which tends to move the sphere in the direction of fluid motion. This force is known as the pressure drag [4].

With increasing N_R transition from a laminar to a turbulent boundary layer occurs and the resulting increased momentum in the boundary layer enables it to continue well past the diametral plane before separation takes place. This results in a reduction of both the wake area and the pressure drag. This transition normally occurs at a value of N_R about 3×10^5 [8]. The value of N_R at transition is called the critical N_R . Figure 2 shows the reduction in drag coefficient C_D resulting from the transition from a laminar to a turbulent boundary layer.

³ See pages 18 and 19, infra.

2C FLOW ABOUT A SPHERICAL MINE CASE

Blunt-nosed bodies with very rough surfaces evidently behave like flat plates or circular discs placed normal to the direction of flow. See Figure 2. They possess no critical point at which drag decreases, i.e., they are independent of N_R . It appears that the boundary layer, be it laminar or turbulent, does not have sufficient momentum to flow completely about a very rough surface. Consequently separation occurs at, or close to the mid-section and drag is practically constant. This is shown in Figure 2 for experiments with one quarter scale models of a spherical mine and also in Figure 3 where the model was a sphere with varying degrees of surface roughness as shown. While neither of the experiments covered the complete range of N_R applicable to moored mines (2×10^5 to 10^6) a critical point can not be expected at higher N_R since turbulence, noise, appendages, and surface roughness all act to lower the critical N_R on a spherical mine.

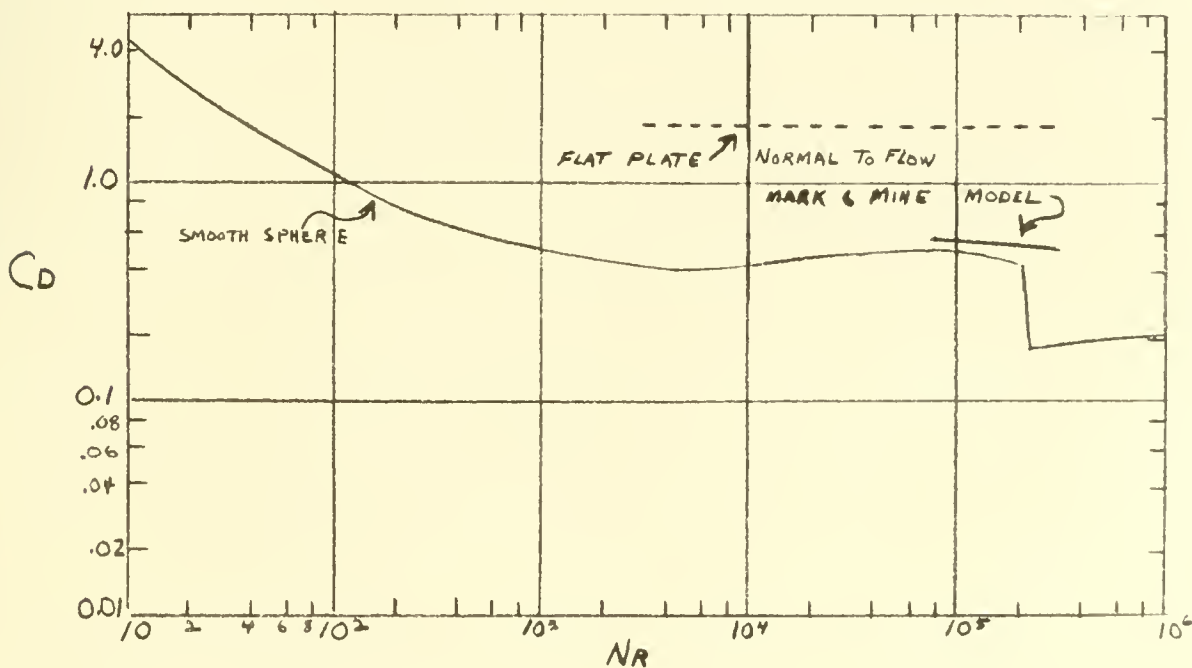


Figure 2 Drag Coefficients for various bodies. Sphere and Flat Plate data from Vennard, reference [1]. Mark 6 Mine model data from NOLM 3024, reference [12].

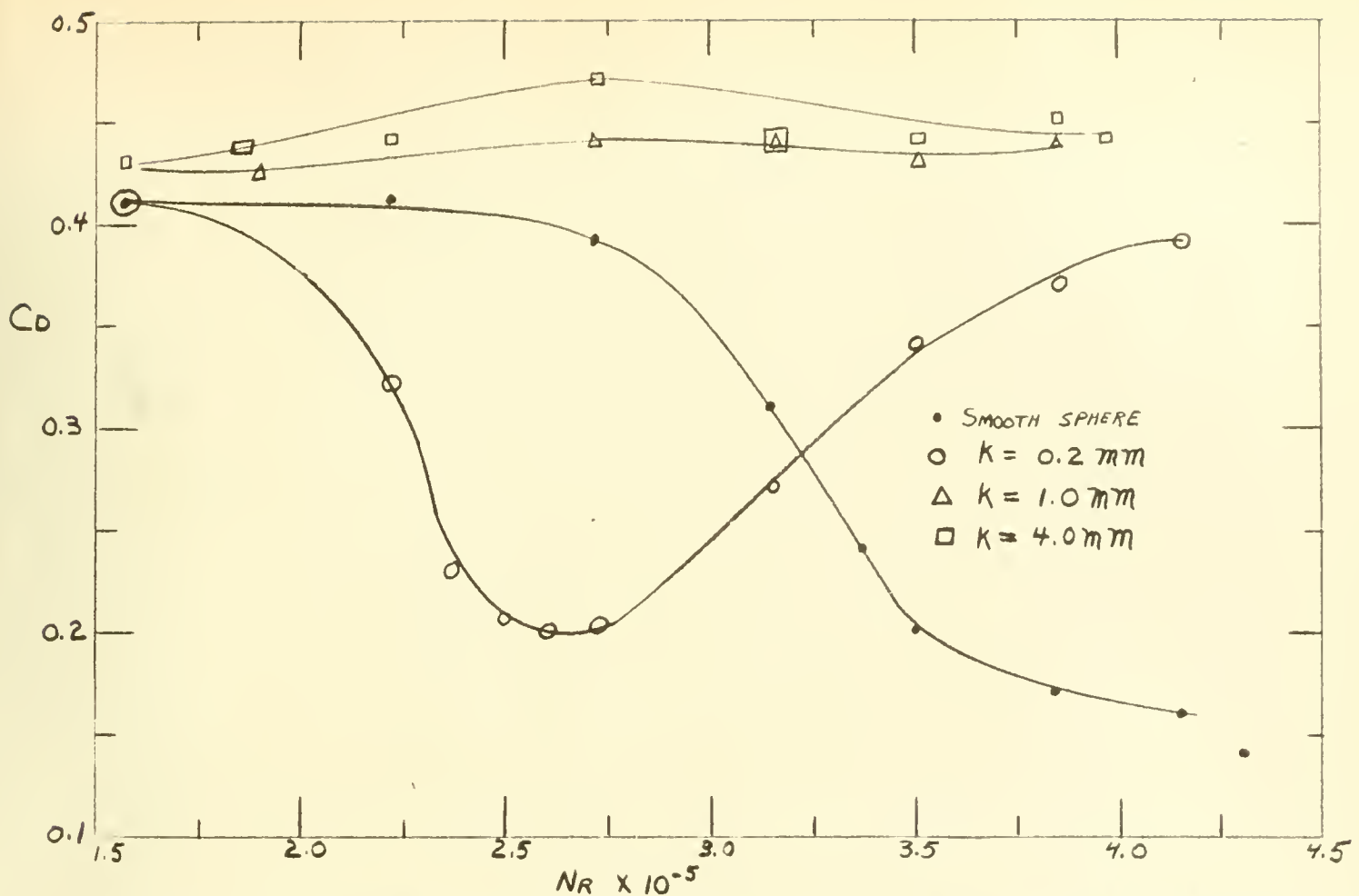


Figure 3 Drag Coefficients for Spheres with varying degrees of surface roughness. (Data from S. Hoerner, Tests of Spheres with reference to Reynolds Number, turbulence, and surface roughness, NACA TM 777)

It is worthwhile to again consider the eddy or vortex formation caused by separation. Winny [9] found that these vortices are shed by a sphere at a frequency of about

$$f_r = \frac{U}{4 d_M}$$

in the N_R range from about 2×10^3 to 4.7×10^4 . The experiments did not extend to higher N_R so it is not known whether this relationship can be applied to moored mines. However, the phenomena may be worthy of investigation if acoustic firing devices are used in moored mines.

2D MINE CABLES

At present, either wire rope or chain is used in mooring U. S. moored mines. Chain, because of its relatively high weight to length ratio, can be used only in shallow water plants. While better suited than wire rope

to endure the bending and twisting suffered by a cable exposed to vigorous water motion it can not be protected with anti-fouling paint [5]. A few representative chain characteristics are presented in Appendix A.

Galvanized wire rope ranging in size from about 7/32 to 1/2 inch in diameter is used in most moorings. While wire rope has the drawback of more drag⁴ and greater susceptibility to failure than chain, these disadvantages are offset by:

1. Smaller weight per length ratio
2. Ease and compactness of stowage as compared to chain
3. Protection by use of anti-fouling compounds.

A few representative wire rope characteristics are presented in Appendix B.

2D1 VORTEX STREET PHENOMENA

Long circular cylinders and similar blunt forms, when oriented with major axis normal to fluid flow, shed eddies alternately from opposite sides. This phenomenon is known as the Karman Vortex Trail or Street and is illustrated in Figure 4.

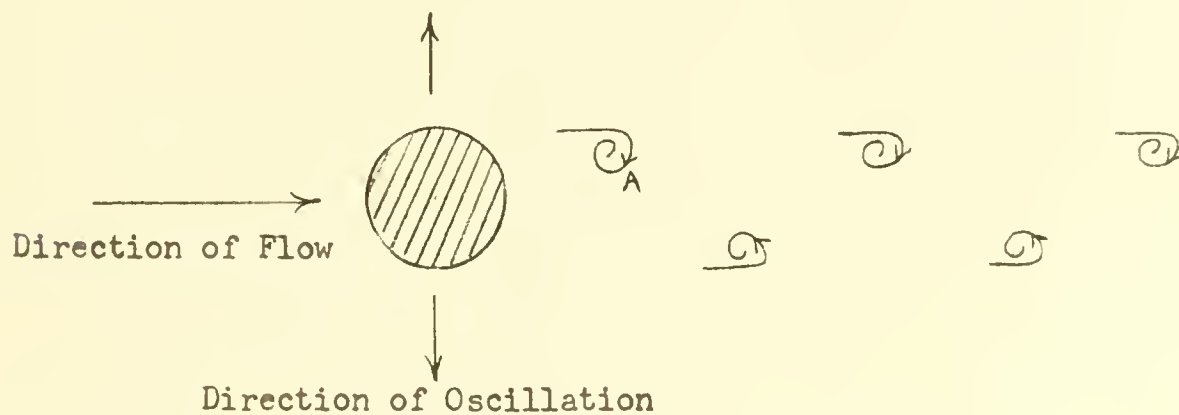


Figure 4 Karman Vortex Street

⁴ See page 17, infra.

Consider the eddy labelled A; due to its rotation a greater instantaneous velocity exists at the upper boundary of the cylinder than at the lower boundary. By Bernoulli's principle, there is a pressure difference between top and bottom of the cylinder, the greater pressure being at the bottom. Thus, we have a force which acts in the upward direction. When this eddy is released the cable will move downward. Another eddy then forms, this time in the lower half of the street. Its direction of rotation is opposite to that of eddy A and the force resulting will be directed downward.

The frequency at which the eddies are shed can be expressed in terms of Strouhal's number N_S

$$N_S = \frac{f_r d}{U}$$

N_S is approximately equal to 0.185 for circular cylinders over the range of N_R for mine cables [10]. For example, a 7/16-inch diameter mine cable exposed to a current of two knots would shed eddies at a frequency

$$f_r = \frac{N_S U}{d} = \frac{0.185(3.28)}{3.64 \times 10^{-2}} = 17.2 \text{ c.p.s.}$$

If this frequency coincides with the natural frequency of the mooring cable the amplitude of oscillation will increase. However, the following factors inhibit large amplitude oscillations in an ocean environment:

1. Possible nonuniformity of velocity over the length of the cable due to a current gradient with depth.
2. A time varying velocity due to wave action.⁵

5 See page 29, infra.

3. Free-stream turbulence

4. Fluid damping

Experiments by NACA [11] have shown that N_S for cylinders of various cross-sectional shapes is approximately equal to 0.2 for subcritical Reynolds Numbers. This is noteworthy in that N_S may be assumed to be approximately constant even though cable shape is changed due to fouling. A correction due to increased diameter would still be necessary, of course.

2D2 MINE-CABLE DRAG COEFFICIENTS

Experiments conducted by the Naval Ordnance Laboratory [12] in an attempt to determine C_D for wire-rope cables with major axis normal to flow produced inconsistent results. This inconsistency was attributed to cable vibration, e.g., cable oscillation of only one to two diameters amplitude increases C_D by a factor of about two. Figure 5, based on a study by NOL of the vortex trail behind a fixed cylinder, indicates that C_D is strongly dependent upon the amplitude of vibration.

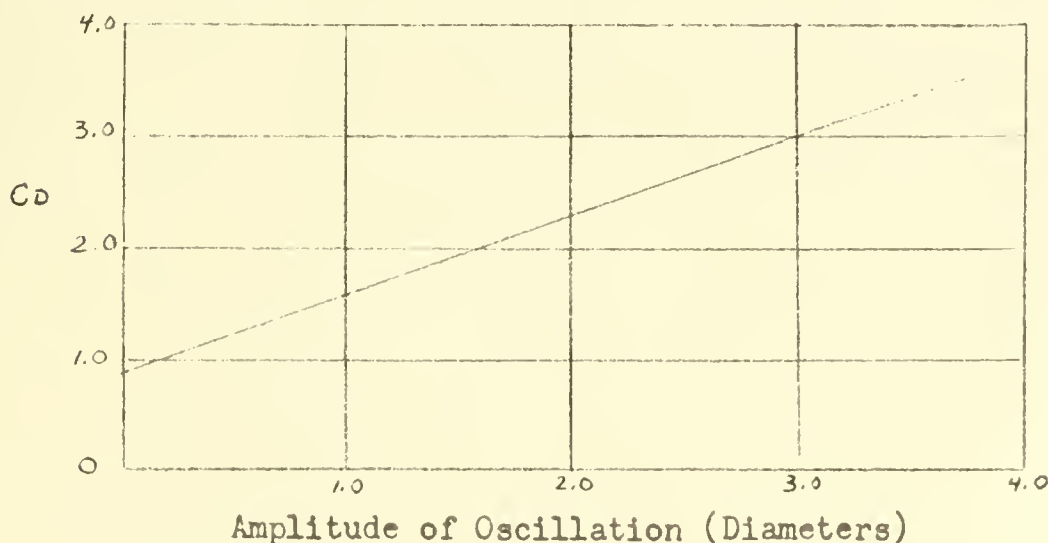


Figure 5 Drag Coefficient versus Amplitude of Oscillating Cylinders. (From NOLM 3024. Reference [12])

When experimental methods failed to produce a usable C_D an indirect approach was used. An empirical C_D was calculated which, when combined with measured mine drag, resulted in a calculated dip approaching the actual dip as found in full-scale tests. This was found to be $C_D = 2.0$.⁶

Based on tests conducted at the David W. Taylor Model Basin [14] the drag coefficient C_D for chain normal to the direction of flow may be taken as approximately equal to 0.91 over the range of N_R applicable to mine mooring chains. The tangential drag coefficient C'_f was found to be 0.085 over the same N_R range. This tangential drag coefficient C'_f was defined as

$$C'_f = \frac{2f'}{d_L U^2}$$

where f' is the tangential drag per linear foot of chain in pounds. All other quantities are as defined in the Table of Notation. It is to be noted that surface area does not enter this equation. This is understandable in the case of a chain.

2E MAGNITUDE OF FRICTIONAL DRAG ON SPHERICAL MINES AND MINE CABLES

In order to arrive at qualitative estimates on the effect of marine growth and to justify the neglect of tangential drag forces on mine cables it is necessary to find the magnitude of the frictional drag force.

6 There is an apparent disagreement between NOL and the David Taylor Model Basin on the value of C_D for wire cables. NOL uses $C_D = 2.0$ and DTMB uses $C_D = 1.5$ [13].

2E1 SPHERICAL MINE

Considering an N_R of 5×10^5 , which is about an average value for a moored mine, the corresponding skin friction drag coefficient (for a turbulent-boundary layer) is approximately $C_f = 0.008$ [6].

The surface area of a smooth spherical mine is given by πd_M^2 . The drag component due to skin friction is then

$$D_f = \frac{C_f}{2} \int \pi d_M^2 U^2$$

The total drag coefficient $C_D = 0.5$ [12] and the projected area normal to flow is $\frac{\pi}{4} d_M^2$. The total drag is then

$$D_T = \frac{C_D}{2} \int \frac{\pi d_M^2}{4} U^2$$

The ratio of drag due to skin friction to the total drag is

$$\frac{D_f}{D_T} = 0.064$$

The drag due to skin friction contributes about six percent of the total drag.

2E2 MINE CABLE

Considering first a wire-rope cable and using⁷ $C_f = 0.01$ [13] and $C_D = 2.0$ [11] we have for a unit length of cable

$$\frac{D_f}{D_T} = \frac{0.01}{2} \frac{\int \pi d U^2}{\int d U^2} = 0.016$$

The drag due to skin friction contributes about two percent of the total drag.

⁷ Calculated from data presented on pages 18 and 19 of DTMB Report 687.

In the case of a unit length of chain cable

$$D_f = \frac{C_{f,d} U^2}{C_{D,d} U^2} = 0.093$$

The tangential drag contributes about nine percent of the total drag.

2F EFFECT OF MARINE FOULING ON DIP

Since the specific gravity of most of the common fouling organisms is about 1.2 to 1.4 [5, 14] the effect of marine growth is manifested mainly in additional drag force rather than increased weight. If the assumptions are made that

1. Skin friction is minor compared to total drag^{8, 9}
2. The mine case and cable are already hydrodynamically rough and an earlier separation will not result from fouling

then the added drag can be computed to a first approximation considering only the increased area due to fouling.

The increase in mine-case diameter due to fouling is limited to approximately six inches. When the layer of marine growth exceeds three inches it tends to break off [15]. An increase in case diameter of six inches would increase the total drag approximately 14 percent.

In contrast with the nominal increase in case drag due to fouling the mere doubling of cable diameter by marine growth doubles the cable drag. In tests conducted by NOL the upper 30 feet of a 1/8 inch cable exposed off Puerto Rico for 40 days accumulated sufficient marine growth to increase its diameter to two inches. In another series of tests

8 See page 18, supra.

9 Each element of marine growth also contributes to the pressure drag, i.e., there can be local separation behind individual growths depending on size and shape. It is tacitly assumed here that added drag generated thereby is negligible. It is the author's opinion that such an assumption is valid for a mine case but questionable for a mine cable.

conducted off La Jolla, California, in 15 feet of water a two to four-fold increase in diameter is apparent from photographs taken of a cable originally of 1/8 inch diameter after three months exposure [13] .

When it is considered that the cable drag force is the chief cause of dip where cable length exceeds about 50 feet the need for cable anti-fouling paint becomes apparent.

2G FORCES ACTING ON A MOORED MINE ASSEMBLAGE

The diagram of the forces acting on a moored mine shown on Figure 6 has been simplified by assuming the mooring cable is a single, stiff, straight rod connected to the mine and anchor with flexible hinges. Certain of the notation used in Figure 6 and the following paragraph is not standard to the rest of this paper. The simplified notation and diagram are presented here in order to discuss certain general features of a mine mooring at this time. Appendix C contains a mathematical analysis of the forces acting on a moored mine exposed to a steady fluid flow.

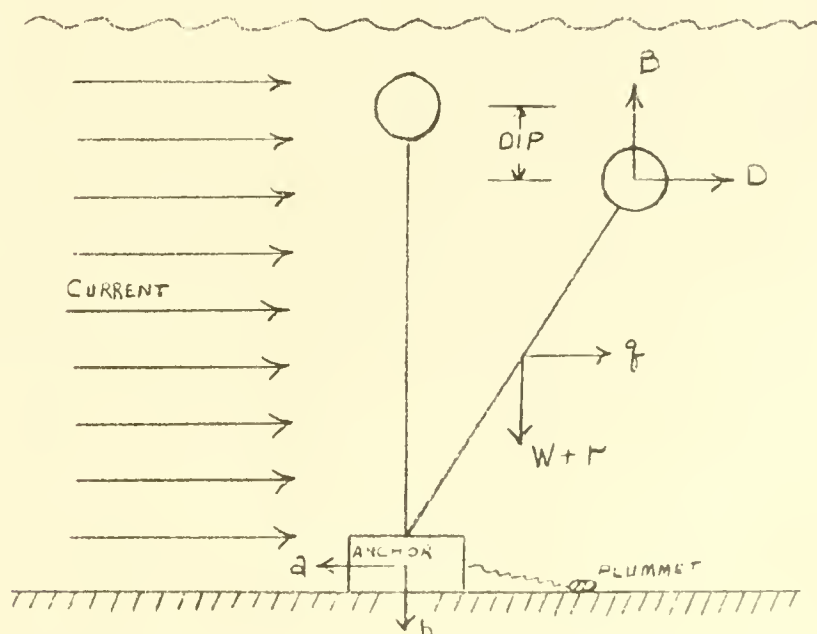


Figure 6 Simplified Diagram of the Forces acting on a Moored Mine

The drag force (D) on the mine case plus the horizontal component of the fluid force on the cable (q) must be balanced by the horizontal component of the anchor resistance (a). Likewise, the buoyant force of the mine case (b) must be equally opposed by the cable weight (W), the vertical component of the fluid force on the cable (r), and the vertical component of the anchor resistance (b).

It is apparent that

1. A decrease in dip can be obtained by:

(a) Increasing mine-case buoyancy. This advantage may be offset by increased drag if the added buoyancy is obtained by increasing case diameter. However, since buoyancy varies as the cube of the case diameter and drag as the square the buoyancy change will predominate.

(b) Utilizing a mine case shaped to produce a lift force when exposed to fluid motion.¹⁰

(c) Streamlining mine case and cable.

(d) Utilizing a lighter weight or smaller mooring cable. It should be observed that methods (a), (b), and (d) above increase the tendency of the mine anchor to walk or slide along the bottom. Methods (a) and (b) may also require the use of stronger and consequently larger cable which may partially offset the advantage gained.

2. The maximum load on the cable is limited by the holding power of the anchor.

10 For example, see U. S. Dept. of Commerce, Coast and Geodetic Survey publication, Roberts Radio Current Meter Mod II by Captain E. B. Roberts, U. S. Coast and Geodetic Survey.

It is profitable to examine the way in which both dip and the force transmitted to the anchor vary in a strong current as cable length increases.

TABLE I

MINE DIP AND FORCES EXERTED ON A MARK 6 MINE
MOORED WITH VARIOUS CABLE LENGTHS IN A STEADY THREE-KNOT CURRENT

<u>Cable Length (Feet)</u>	<u>Dip (Feet)</u>	<u>Horizontal Force Exerted on Anchor (Lbs)</u>	<u>Vertical Force Exerted on Anchor (Lbs)</u>	<u>Total Force Exerted on Anchor (Lbs)</u>
50	5	158	231	280
100	17	197	183	270
150	37	219	142	261
200	62	230	109	254
250	93	235	82	250
300	127	238	60	246
350	167	239	46	244
400	208	240	30	242
450	254	240	16	240
500	304	240	2	240

This table was constructed using the method as outlined in Appendix C, example number two. It is unlikely that a steady-three knot current would extend to a depth of 500 feet. The table was extended to this depth to demonstrate the behavior of this configuration in a strong current as depth and cable length increase.

Table I shows that as cable length increases

1. Horizontal pull on anchor increases, but not excessively.
2. Vertical pull on anchor decreases, becoming negligible for long cable lengths.
3. The rate of increase of the horizontal anchor force is less than the rate of decrease of the vertical pull on the anchor. Thus, the total force on the anchor decreases slowly with increasing cable length until a "critical length" is reached. At depths exceeding the critical length part of the cable is resting on the bottom and the anchor force becomes virtually constant. In the case considered the critical length is reached when the cable is between 450 and 500 feet long.
4. When the critical length is reached severe cable abrasion on the sea floor can be expected for rough, hard-bottom materials.
5. Dip increases rapidly.

2H HOLDING POWER OF MARK 6 ANCHOR

In U. S. Mark 6 type mines the anchor is a rectangular steel box about 2.5 feet square and two feet in height. This anchor holds by virtue of weight alone unless it sinks into the bottom. If it sinks a force in addition to the normal friction force, which might be termed "plowing" resistance, must be exerted to move the anchor in a horizontal direction. The plowing resistance is due to the resistance of the bottom material to movement,¹¹ which in turn is a function of the shear strength and density of the bottom material. In the vertical direction a suction force would probably be added to the gravity force.

¹¹ Skin friction between the sides of the anchor and the bottom material has been neglected here since it is small compared to the other forces.

Experimental data pertaining to Mark 6 anchor-holding power in various type bottoms is not available. It may be assumed, however, that holding power is at a minimum if the mine is exposed on any type of smooth, sloping, hard bottom, and at a maximum if buried in a mud bottom. Table II is a tabulation of the probable behavior of a block-type anchor in various types of bottoms. The holding power ratings listed represent opinions of the author only.

In order to arrive at a qualitative estimate of the magnitude of a steady current required to cause movement of a Mark 6 mine anchor consider the mine for which values of the anchor forces are presented in Table I and assume

1. The mine is planted on a flat, hard bottom such as rock, sand, or compacted clay, and no anchor penetration has occurred.
2. The plummet's resistance can be neglected compared to the anchor resistance.
3. The anchor will either walk or slide along the bottom rather than overturn. (See Appendix D)

The weight W_A of a Mark 6 anchor in water is approximately 709 lbs.

The effective weight is the weight of the anchor in water minus the upward pull of the cable Y_A . The horizontal pull on the anchor exerted by the cable is X_A . If the coefficient of friction μ between the anchor and the bottom sediment is less than

$$\mu_{\text{crit}} = \frac{X_A}{W_A - Y_A}$$

then the anchor may slide along the bottom.

Calculations using the data in Table II result in values of μ_{crit} between 0.3 and 0.4 for all cable lengths. It can be assumed then that if μ between the bottom and a Mark 6 anchor is less than 0.3 sliding will occur. If μ is between 0.3 and 0.4 sliding may occur and if μ is greater than 0.4 the anchor will hold. The values given above are for a three-knot current. For a current speed of four knots μ_{crit} is between 0.4 and 0.5.

TABLE II

BEHAVIOR OF MARK 6 TYPE ANCHOR IN DIFFERENT BOTTOM TYPES

<u>BOTTOM TYPE</u>	<u>PENETRATION</u>	<u>RESISTANCE TO SLIDING MOTION</u>	<u>EFFECT OF BOTTOM SLOPE</u>	<u>REMARKS</u>	<u>HOLDING POWER RATING</u>
Rock or coral	None	Low on smooth bottoms but may be high on irregular bottoms. Irregularities more extreme and more prevalent on coral bottoms.	Holding power very poor on smooth bottoms. Little or no effect on irregular bottoms.	Anchor may become lodged in crevices or other irregularities becoming virtually fixed in place.	Poor on smooth bottom. Good on rough rock and coral ¹² bottoms.
Hard clay	Little or none	Low	Decreases holding power		Fair
Sand	Little or none on incompact. Anchor may become buried with time due to scouring action of water currents	Moderate	Decreases holding power	If anchor is not moved within first few weeks after immersion it probably will not move thereafter.	Fair (Better than hard clay)
Soft mud, clay, or silt	Depth of penetration will depend on sediment strength		Very little influence	Case depth probably lower than set depth due to penetration.	Very good ¹³

- ¹² On a coral bottom the anchor may move only a small distance but the erratic case depths obtained using the plummet controlled depth setter in a Mark 6 mine, due to the irregular depths typical of coral bottoms, would make the use of a different type mine advisable
- ¹³ Mud, while providing good holding ground, may be poor from a tactical viewpoint if case depth setting is at all critical. This situation could arise, for example, off the mouth of a river where a thick layer of weak, uncompacted mud may cover the bottom. In such locations an anchor may sink several feet.

CHAPTER 3

OSCILLATORY FLOW FORCES

The objective of this chapter is to examine the forces exerted on a moored mine assemblage due to ocean waves.

3A WAVE MOTION

The equations used to describe progressive¹ wave motion herein are taken from a publication² on waves issued by the Beach Erosion Board [16]. They are strictly applicable only under the following special conditions.

1. Wave profile is sinusoidal in form.
2. Wave height is small compared to wave length. (This ratio is usually called wave steepness).
3. Wave height small compared to water depth.

However, they describe motion accurately enough for engineering calculations, except

1. In and near the breaker zone.
2. For steep³ waves in very shallow water⁴.
3. For very steep waves in any water depth.

Since moored mines are seldom used in the breaker zone or in very shallow water these equations are applicable in most moored mine problems.

- 1 The term progressive refers to a wave in which the wave form moves in the direction of propagation.
- 2 Some minor changes have been made in notation.
- 3 Steepness is defined as the ratio of wave height to wave length.
- 4 Very shallow water is defined as that where the depth of water is less than 1/50 of a wave length.

Very steep waves may be encountered in active storm areas, and then the use of these equations will result in calculated forces which are smaller than the actual forces.

3A1 WAVE NOMENCLATURE AND DEFINITIONS

Symbols used in the following equations are defined in the Table of Notation at the beginning of this paper.

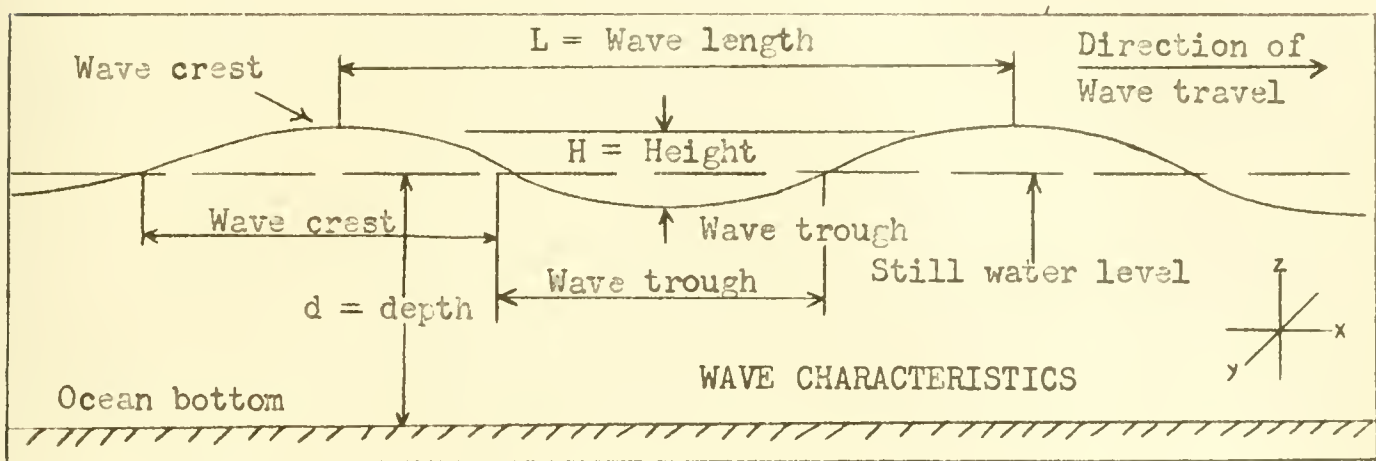


Figure 7 Wave Nomenclature. (From Special Issue No. 2, Bulletin of the Beach Erosion Board, Dept. of the Army, Corps of Engineers)

The basic relationship between wave length, celerity, and period for periodic motion is

$$L = CT$$

WAVE CELERITY OR VELOCITY OF PROPAGATION - Neglecting a surface-tension term, which is negligible in the case of ocean waves that have lengths exceeding a few inches, the velocity of a progressive wave on the sea surface in any water depth is

$$C^2 = \frac{g}{K} \tanh Kh$$

WAVE LENGTH - The wave length L , i.e., the horizontal distance from crest to crest, obtained by a simple substitution in the foregoing equations, is

$$L = \frac{gT^2}{2\pi} \tanh Kh$$

WAVE HEIGHT - The wave height H is the vertical distance from crest to trough.

SURFACE PROFILE - The shape of the surface profile can be obtained from

$$\eta = \frac{H}{2} \cos (Kx - \sigma t)$$

PARTICLE DISPLACEMENT - The horizontal and vertical displacements, ξ and ζ , respectively, of a water particle from the mean position it would occupy in the absence of waves, are

$$\xi = -\frac{H}{2} \frac{\cosh K(h+Z)}{\sinh Kh} \sin (Kx - \sigma t)$$

$$\zeta = \frac{H}{2} \frac{\sinh K(h+Z)}{\sinh Kh} \cos (Kx - \sigma t)$$

In these expressions the hyperbolic functions represent a damping factor. Z is negative downward and h is always positive.

PARTICLE VELOCITY - The horizontal and vertical components of particle velocity u and w , respectively, are obtained by differentiation of the equations for particle displacement with respect to time.

$$u = \frac{Hg}{2} \frac{\cosh K(h+Z)}{\sinh Kh} \cos (Kx - \sigma t)$$

$$w = \frac{Hg}{2} \frac{\sinh K(h+Z)}{\sinh Kh} \sin (Kx - \sigma t)$$

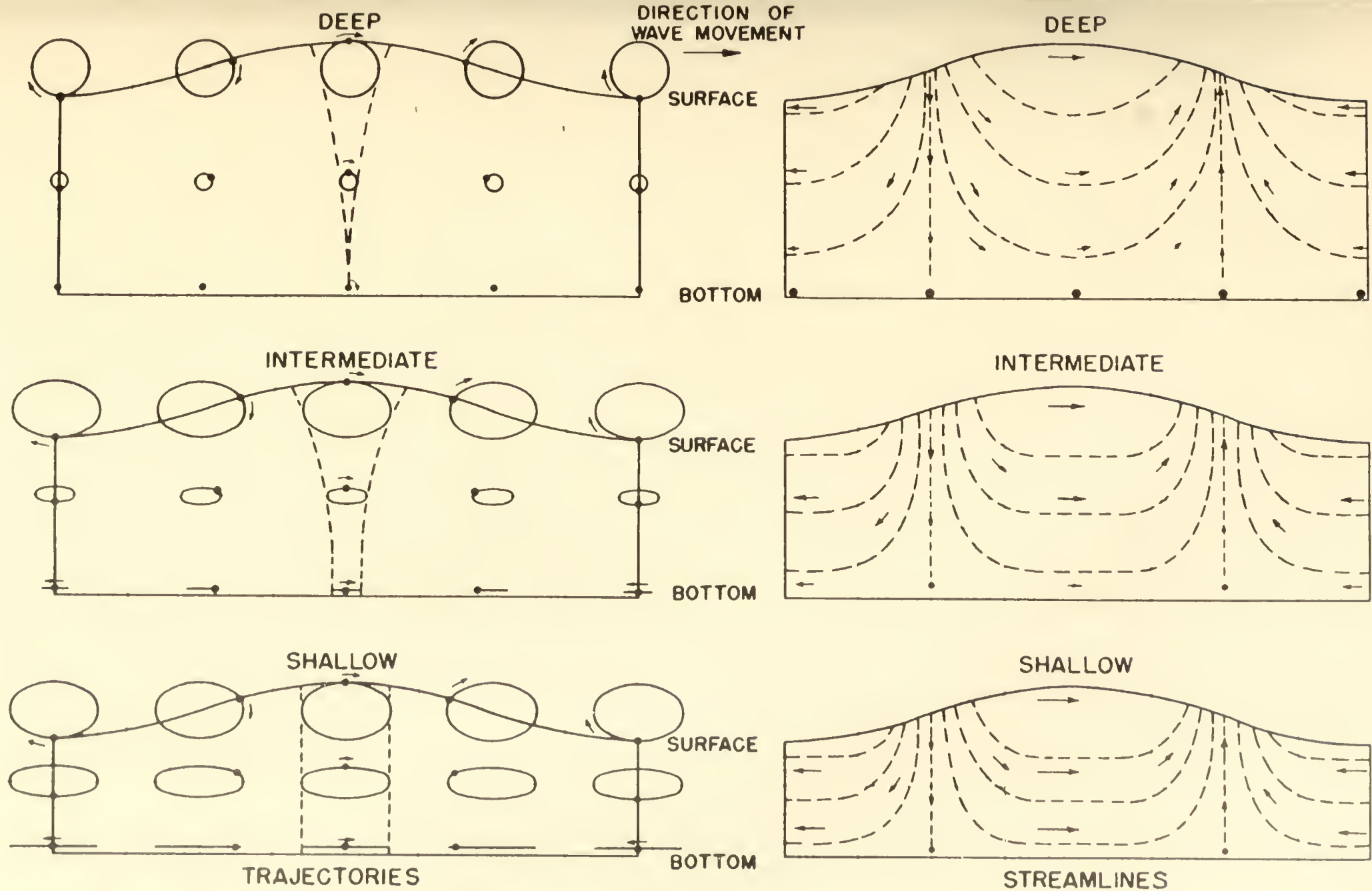


FIGURE 8 TRAJECTORIES AND STREAMLINES OF PARTICLE MOTION IN A PROGRESSIVE WAVE.

(ARROWS INDICATE DIRECTION OF MOVEMENT)

PARTICLE ACCELERATION - The horizontal and vertical components of particle acceleration, $\frac{\partial u}{\partial t}$ and $\frac{\partial w}{\partial t}$, respectively, are obtained by a second differentiation of the equations for particle displacement with respect to time.

$$\frac{\partial u}{\partial t} = \frac{Hg^2}{2} \frac{\cosh K(h+Z)}{\sinh Kh} \sin (Kx-\sigma t)$$

$$\frac{\partial w}{\partial t} = - \frac{Hg^2}{2} \frac{\sinh K(h+Z)}{\sinh Kh} \cos (Kx-\sigma t)$$

It should be noted that in both differentiations the implicit assumption has been made that ξ and ζ represent displacements of a particle from its equilibrium or mean position.

3A2 DEEP-WATER WAVES

The ratio of the water depth to wave length in deep water is called the relative depth. If the relative depth is greater than 1/2, certain of the general equations given in the preceding section can be simplified. The general expression for wave velocity can be written

$$C^2 = \frac{g}{K} \tanh Kh$$

When $\frac{h}{L_0} \geq \frac{1}{2}$, $\tanh Kh \doteq 1$, and the above expression is approximated

by

$$C_0^2 = \frac{gL_0}{2\pi} = 5.12L_0$$

when C_o is in ft/sec., L_o is in feet and T is in seconds. The subscript, o, indicates the value of the parameter in deep water. Further,

$$C_o = 5.12T$$

and

$$L_o = 5.12T^2$$

which indicates that, in deep water, wave velocity and wave length are independent of water depth.

In deep-water waves the particle orbits are circular. The diameter of the orbital circle at the surface is equal to the wave height and decreases exponentially with increasing depth. Each particle completes a circular transit once each wave period, particles at the wave crest moving in the direction of wave progress. At the surface, then, a particle must travel a distance πH feet every wave period, which means that particle velocity is directly proportional to wave height and inversely proportional to wave period. Figure 8 shows the trajectories and also the instantaneous velocities of water particles in relation to wave phase. Table III shows the rapid decrease in orbital diameter and particle velocity with depth.

It is apparent that

1. As wave length and wave height increase, the depth to which appreciable orbital motion penetrates is increased.
2. Wave energy is concentrated close to the sea surface. Because of this rapid decay with depth, and because of the small diameter

of the cable necessarily used in deep-water mine moorings (to allow positive buoyancy) it is assumed here that wave forces on cables in deep water can be neglected.

TABLE III

ORBITAL DIAMETER AND PARTICLE VELOCITY AS A FUNCTION OF DEPTH IN A DEEP-WATER WAVE

Depth (ft)	0	$0.1L_0$	$0.2L_0$	$0.3L_0$	$0.4L_0$	$0.5L_0$	$0.75L_0$	L_0
Orbital Diameter (ft)	H	0.53H	0.28H	0.15H	0.08H	0.04H	0.009H	0.002H
Particle Velocity (ft/sec.)	$\frac{\pi H}{T}$	$\frac{1.67H}{T}$	$\frac{0.9H}{T}$	$\frac{0.48H}{T}$	$\frac{0.25H}{T}$	$\frac{0.14H}{T}$	$\frac{0.03H}{T}$	$\frac{0.006H}{T}$

3A3 SHALLOW-WATER WAVES

When the depth of water is less than $1/25$ of the deep-water wave length the water is referred to as shallow. Certain of the general equations given in section 3A1 can then be simplified. When $\frac{h}{L}$ is small, $\tanh kh = kh$; and the general expression for wave velocity becomes

$$C_s = \sqrt{gh}$$

where the subscript, s, indicates the value of the parameter in shallow water only. The equation shows that wave velocity is independent of either wave length or period (in contrast to deep-water waves) but is proportional to the square root of the water depth.

Further, the wave length in shallow water is

$$L_s = T \sqrt{gh}$$

In shallow water vertical particle motion is impossible at the bottom and as a consequence particles at the bottom merely surge back and forth as a wave passes. At the surface the boundary restriction interferes less with particle motion and the orbit is elliptical with its major axis horizontal as shown in Figure 8.

Examination of the damping functions for particle displacement is instructive. The horizontal particle displacement is in the general case

$$\xi = \frac{H}{2} \frac{\cosh K(h+z)}{\sinh Kh} \sin (Kx - \sigma t)$$

For small values of $K(h+z)$ as are found in shallow water, $\cosh K(h+z)$ approaches unity; and for small values of Kh , $\sinh Kh$ approaches Kh . Therefore,

$$\xi = - \frac{HL}{4\pi h} \sin (Kx - \sigma t)$$

or in words, the horizontal particle motion is proportional to the wave height and length, inversely proportional to depth, and is not attenuated with depth below the surface.

The vertical particle displacement is in the general case

$$\zeta = \frac{H}{2} \frac{\sinh K(h+z)}{\sinh Kh} \cos (Kx - \sigma t)$$

For small values of $K(h+z)$ and Kh the damping function $\frac{\sinh K(h+z)}{\sinh Kh}$ approaches $1 + \frac{z}{h}$. Since z is negative in the direction of increasing depth it is evident that vertical damping is linear with increasing depth. The vertical particle displacement simplifies to

$$\zeta = \frac{H}{2} \left(1 + \frac{z}{h}\right) \cos (Kx - \sigma t)$$

which is dependent upon wave height but independent of wave length.

The absence here of wave length, which is ordinarily a large value, and its inclusion in the numerator of the equation for horizontal particle motion shows that vertical motion is small compared to horizontal. Consequently, only oscillatory flow forces due to horizontal particle motion need be considered in shallow water.

It should be noted that only waves of long period and great length will be classified as shallow-water waves within the depth range practical for moored mines. For example, at a depth of 50 feet, which would be considered close to the inshore-depth limit for a moored mine, only waves with periods exceeding 15.6 seconds and deep-water length over 1250 feet could be classed as shallow water waves. If the water is 100 feet deep the required period and deep-water length would be 22 seconds and 2500 feet, respectively. Thus, most mines will be in water classified as intermediate or deep with respect to ocean waves.

3A4 TRANSITIONAL WAVES

Transitional or intermediate-depth waves are those which can not be classed as either deep or shallow water waves. Their characteristics depend upon both wave length and water depth, hence the general wave equations apply. The general equations, however, can not be used conveniently in the form presented in article 3A1. So they have been combined with the deep-water simplified equations in such a way as to give the following equations for wave speed and length [18] .

$$\frac{c}{c_0} = \tanh Kh$$

$$\frac{L}{L_0} = \tanh Kh$$

These expressions are plotted in graphical form in Figure 9 which also gives shallow and deep-water wave speed and length.

Particle motion in transitional waves is intermediate between that in deep and shallow-water waves. Orbits of water particles are elliptical with the major axes horizontal as shown in Figure 8. The attenuation of particle motion with depth is less than that in deep water and greater than that in shallow water.

3B FORCES DUE TO OSCILLATORY FLOW

In what follows in this section it is assumed

1. The size of the mine case and cable segments are so small relative to the wave length that particle motion can be considered to vary only with time in the region they occupy.
2. Steady current forces are zero.

3B1 DRAG FORCE

The drag force in oscillatory flow as in steady flow is a result of viscous friction. The total drag force on a submerged object was previously⁵ expressed as

$$D_T = \frac{1}{2} C_D \int AU^2$$

In oscillatory flow the velocity term used will be the velocity of water particles as they move in response to a progressive surface wave. Possible changes in C_D due to oscillatory flow are discussed in the following paragraph. The other factors are identical in both steady and oscillatory flow.

⁵ See page 4, supra.

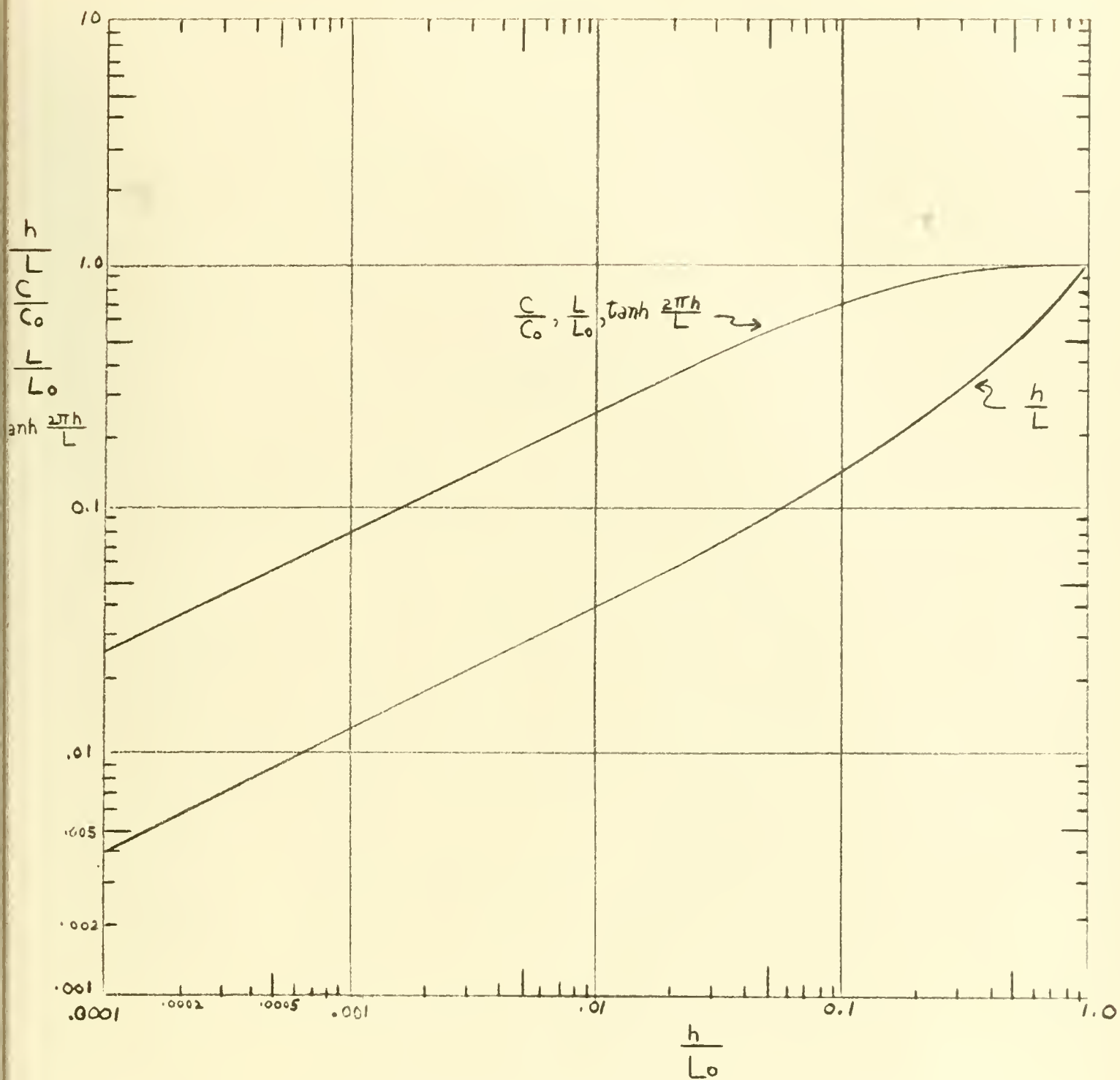


Figure 9 Illustration of Various Functions of Kh. (From Special Issue No. 2, Bulletin of the Beach Erosion Board, Dept. of the Army, Corps of Engineers)

3B1A DRAG COEFFICIENTS IN OSCILLATORY FLOW

In oscillatory flow about blunt-nosed objects at low N_R the drag coefficient C_D is usually somewhat higher than C_D in steady flow. At N_R exceeding 10^4 , however, C_D in both type flow conditions appears to converge in the case of a sphere [19]. When there is significant drag on a sphere three feet in diameter N_R exceeds 10^4 ; therefore, in this paper a constant C_D of 0.5 will be assumed for mine cases.

In the case of mine cables direct experimental data is lacking. Morison, et.al., [20] found a C_D of 1.63 ± 0.41 for upright circular pier piling normal to oscillatory flow in the N_R range 2200 to 11000. Since C_D for smooth circular cylinders in steady flow is normally about 1.1 in this N_R range it would seem that oscillatory flow increases the drag force. The magnitude of this increase indicates it can not be attributed solely to possible surface roughness of the piles.

A more complex situation exists with a vibrating cable in oscillatory flow than with a fixed piling. As previously shown⁶ cable oscillation increases the drag coefficient. The dual effect, then, of cable and fluid oscillation may be to increase the drag coefficient above the value of 2.0 used for steady flow conditions. However, a C_D of 2.0 was chosen as that which best fitted actual conditions of full-scale mine dip tests in Puget Sound [21]. While wave conditions are not mentioned in the report it may be assumed some wave motion was present.

⁶ See page 16, supra.

Since no experimental data are available it would seem that a C_D of 2.0 is the best available estimate and that value will be used herein as the drag coefficient for mine cables in oscillatory flow.

3B2 INERTIAL FORCE

When an object is accelerated in a vacuum a force must be exerted which is proportional to its mass. The equation representing this force is usually written in the form

$$F = M \frac{du}{dt}$$

If the same object is accelerated in a fluid medium an additional force is necessary to produce the same acceleration since the object necessarily displaces and accelerates some of the fluid in its movement. This loss of kinetic energy to the fluid is customarily accounted for by considering the accelerated object as having an added or virtual mass. The magnitude of this virtual mass, being dependent upon the amount of fluid set in motion by the object, is a function of its geometry and the state of flow [22]. For example, a streamlined object would carry very little of the fluid along with its travel. A blunt form on the other hand would set a larger mass of fluid in motion. Intuitively it would seem that at N_R exceeding 1000 a sphere would probably carry along little fluid until separation occurred, then it may have to drag along the mass of fluid contained in its wake. At the present time the correlation, if any, between N_R and virtual mass has not been demonstrated experimentally. In fact, in experiments with spheres O'Brien and Morison found no correlation between N_R and virtual mass over the N_R range from 1000 to 8000 [19].

Taking into account the virtual mass, the total force to give the body an acceleration $\frac{du}{dt}$ is

$$F = (M + qM') \frac{du}{dt}$$

where q represents a coefficient determined experimentally, M' is the mass of the fluid displaced by the object and M is the mass of the object. In the case of a sphere q is theoretically equal to 0.5 [23].

If the mine case and cable are regarded as fixed while the fluid moves then the fluid is retarded. In order to change to momentum of the fluid a force is required. By Newton's third law an equal and opposite force is exerted by the fluid on the fixed body; this force is proportional to the rate of change of momentum of the fluid. The fluid mass retarded is equal to that displaced by the fixed body plus an additional amount dependent upon flow conditions. We can then represent the mass of retarded fluid by a factor of the type

$$C_M \int V$$

and we have

$$F = C_M \int V \frac{du}{dt}$$

The coefficient of mass C_M for a sphere is theoretically 1.5. Experimentally Morison and O'Brien found an average value of 1.59 for spheres [19] and Morison et.al., obtained a value of 1.51 ± 0.20 [20] for cylindrical piling which is of the same form as a mine cable. A C_M of 1.5 will be used herein for both mine cases and cables.

Neglecting second order terms which are of small magnitude,

$$\frac{\partial u}{\partial t} = \dot{u}$$

in an ocean wave and we have for the horizontal and vertical inertial force equations

$$F_H = C_M \int V \frac{\partial u}{\partial t}$$

$$F_V = C_M \int V \frac{\partial w}{\partial t}$$

3B3 MOTION OF A MOORED MINE CASE

In the following treatment these general assumptions are made:

1. The mine case is fixed below the sea surface by a relatively light, flexible, elastic cable, to the other end of which is affixed a heavy anchor.
2. The depth of submergence of the mine case is such that its presence does not influence the surface profile.
3. In the absence of oscillatory forces the mine is directly above the anchor, i.e., there are no steady current forces.
4. Oscillatory flow forces on the cable are very small and can be neglected.⁷
5. All forces both internal and external act through the geometric center of the mine case which is at the origin of the coordinate system shown in Figure 10.

In addition to these general assumptions additional assumptions pertaining to the particular type of motion under consideration may be made hereafter.

⁷ See page 51, infra.

A mine moored in the preceding fashion is capable of movement with six degrees of freedom, translation in any of three directions and rotation about any of the three axes.

Considering the positive x - axis as the direction of wave advance and borrowing from the nomenclature used in describing ship motion, these motions can be described as follows:

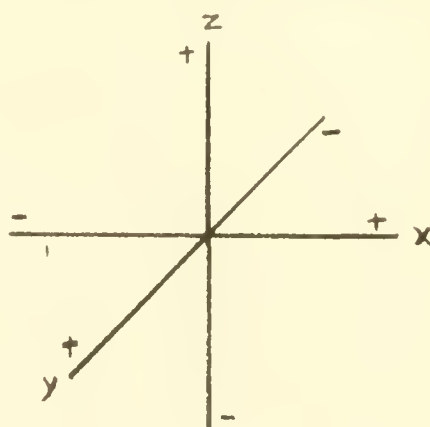


Figure 10 Coordinate system

SURGING - Motion fore and aft in the direction of wave advance.

SWAYING - Motion "to and fro" in direction transverse to wave direction.

HEAVING - Motion up and down.

ROLLING - Angular rotation about the x-axis.

PITCHING - Angular rotation about the y-axis.

SPINNING - Angular rotation about the z-axis.

The three modes of rotation are going to be neglected herein as minor sources of energy dissipation compared with the energy dissipated in translation.

The following analysis was made in order to determine the response of a moored mine to an intermittent or periodic disturbing force. An attempt is made to determine whether resonance can occur between a moored mine and the periodic disturbing force due to uniform ocean waves. In what follows the additional assumption is made that surging, swaying, and heaving are entirely independent of each other. It will be shown that

the natural heaving frequency is much higher than the natural surging and swaying frequencies which means that the heaving motion can exist practically independent of the others. Further, the effect of particle motion in uniform waves is favorable to surging rather than swaying. Thus, it can be stated that surging motion is practically independent of swaying.

HEAVING - Consider the mine mooring shown in Figure 11.

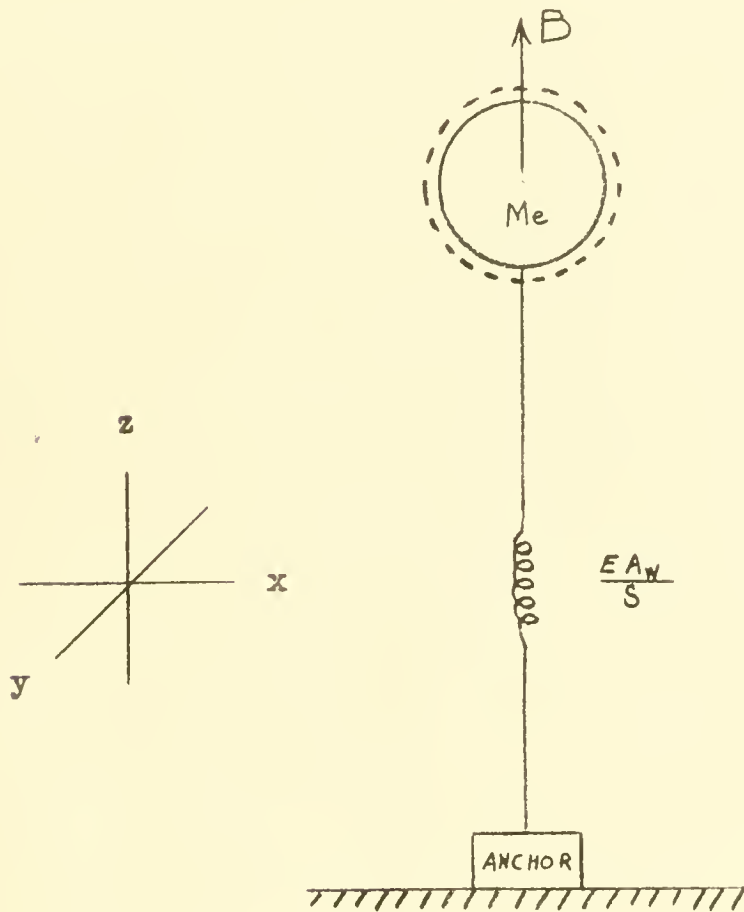


Figure 11 Idealized scheme of moored mine with a fictitious spring representing the effective spring constant of the wire rope cable

Consider this as a normal spring loaded mass-vibratory system and make the following assumptions:

1. The effective mass M_e of the system is composed of the mine-case mass M and its virtual mass qM plus the mass M_c of that portion (assumed to be one third) of the mine cable which acts as part of the oscillatory mass. This neglects the virtual mass associated with the cable which is small compared to the effective mass of the system.
2. The effective mass of the system is contained in a small area about the geometric center of the spherical mine case.
3. Frictional damping effects are small. It has been found both theoretically [23] and in experiments [4] with oscillating pendulums in fluid mediums that the added mass due to the virtual mass effect has a much greater influence on the period than frictional damping.

An approximate solution for the natural heaving period can be obtained from the following differential equation

$$M_e \frac{d^2 z}{dt^2} + \frac{EA_w}{S} z = B$$

Solving for the period

$$T = 2\pi \sqrt{\frac{SM_e}{EA_w}}$$

Table IV shows approximate natural heaving periods for Mark 6 mines moored with wire rope cable of certain diameters and lengths. See Appendix E for a sample computation.

TABLE IV

APPROXIMATE NATURAL HEAVING PERIOD OF MARK 6 TYPE MINE

<u>Cable Diameter (Inches)</u>	<u>Cable Length (Feet)</u>	<u>Natural Heaving Period (Seconds)</u>
7/16	100	0.4
7/16	300	0.6
7/16	500	0.8
7/16	700	1.0
5/16	1000	1.6
1/4	1500	2.5
1/4	2000	2.9

It is evident that resonance would occur in the fundamental mode only with mines having very long cables responding to short-period waves. In an actual ocean wave spectrum there will usually be some waves with such short periods. However, the particle motion due to these waves penetrates only a short distance below the surface. For example, a three-second wave in deep water has a wave length of about 45 feet. Particle movement at a depth of five feet is only about 50 percent of the surface particle movement and for all practical purposes the water is not disturbed below a depth equal to the wave length. It can be concluded then that resonance effects in heaving motion would be rare.

In heaving motion the forces resisting mine movement are relatively large. The buoyant force resists displacements in the negative z direction and what amounts to a very stiff spring attached to a heavy anchor resists upward displacement. These relatively large restraining

forces plus the rarity of resonance permits computation of the oscillatory forces in the vertical direction based on the assumption that the mine is fixed in space as far as vertical motion is concerned.

SURGING - In order to derive the differential equation for surging motion consider Figure 12 showing a mine case which has been displaced a small distance ϵ from its equilibrium position. Assume

1. All forces act through the geometric center of the mine case.
2. ϵ is very small compared to S .
3. The mass of the system is composed of the mass of the mine case M and its virtual mass qM' . This neglects the mass and virtual mass of that portion of the cable which acts as part of the oscillatory mass. However, this is a small quantity compared to $M + qM'$.
4. The mass of the system is centered in a small area about the geometric center of the spherical mine case.
5. Frictional damping effects are small.⁸

The buoyant force B can be resolved into components parallel and perpendicular to the mooring cable. There being no acceleration in the direction parallel to the cable, the component of the buoyant force in this direction must be equal and opposite to the cable tension T_e . The resultant force on the mine case is R .

⁸ See page 42, supra.

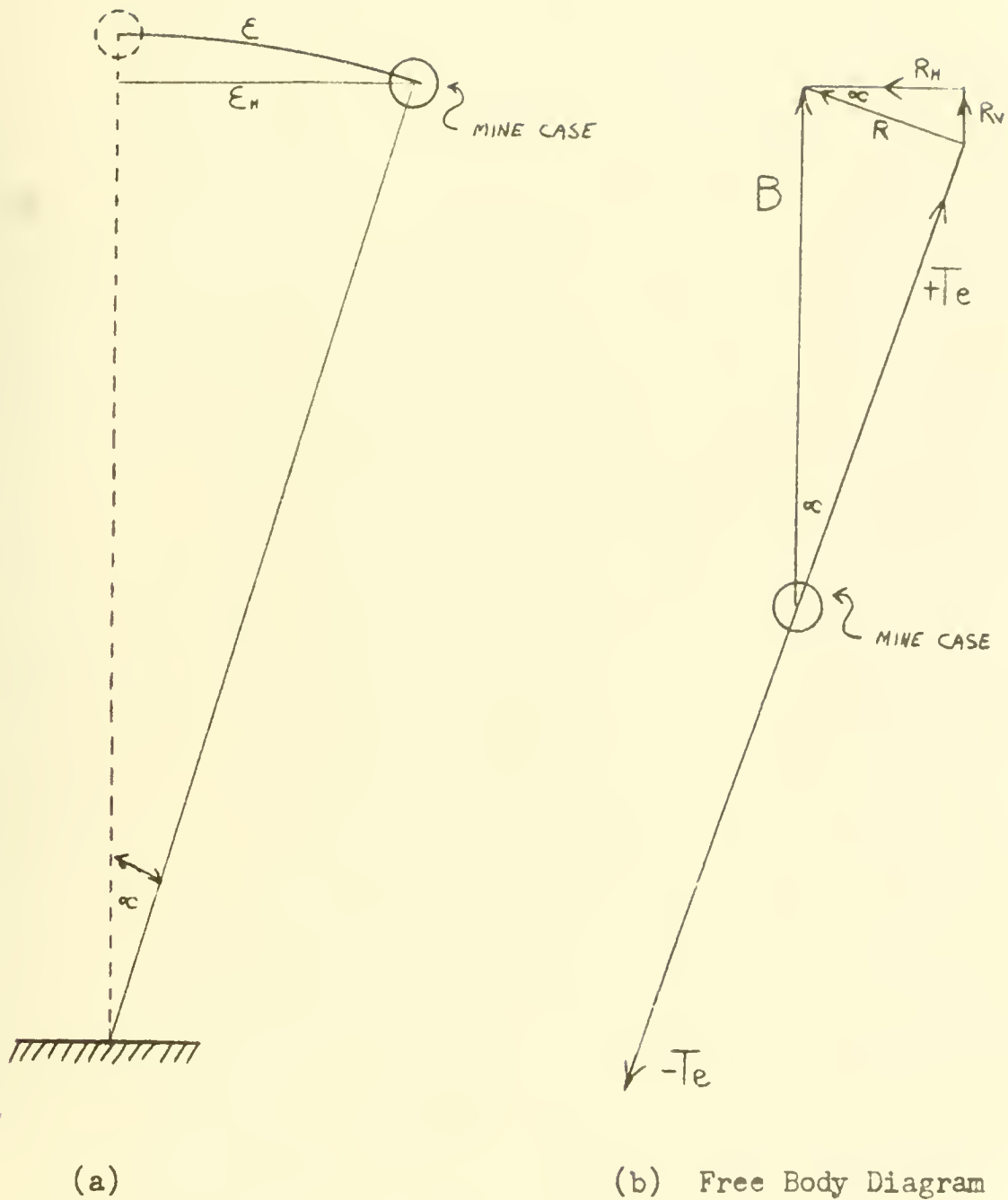


Figure 12 Mine case displaced a small distance from its equilibrium position

The horizontal component of R is

$$R_H = R \cos \alpha = B \sin \alpha \cos \alpha$$

For small α

$$\dot{\epsilon} = S \alpha$$

$$\sin \alpha = \alpha$$

$$\cos \alpha = 1$$

$$\epsilon_H = \epsilon$$

Thus,

$$R_H = \frac{B \epsilon_H}{S}$$

giving a horizontal restoring force which is proportional to the horizontal displacement.

The vertical component of R is

$$\begin{aligned} R_V &= R \sin \alpha = B \sin^2 \alpha \\ &= B \left[\frac{\epsilon_H}{S} \right]^2 \end{aligned}$$

To demonstrate the magnitude of these forces a numerical example will be used. If a Mark 6 mine with $B = 283$ lbs, moored with 500 feet of cable, is displaced horizontally a distance $\epsilon_H = 5$ feet,⁹ then

$$R_H = \frac{283(5)}{500} = 2.83 \text{ lbs}$$

$$R_V = 283 \left(\frac{5}{500} \right)^2 = 0.0283 \text{ lbs}$$

9 This is equivalent to the horizontal particle displacement close to the surface resulting from the passage of a wave ten feet in height.

It is clear that R_V is very small compared to R_H and consequently it will be neglected hereafter.

An approximate solution for the natural surging period can be found from the following differential equation:

$$(M+qM') \frac{d^2x}{dt^2} + \frac{B}{S} x = 0$$

Solving for the period,

$$T = \frac{2\pi}{\sqrt{\frac{B}{S(M+qM')}}}$$

Table V shows approximate natural surging periods for a Mark 6 mine moored with various cable lengths. Appendix F shows the characteristics of the mine considered and a sample computation.

TABLE V
APPROXIMATE NATURAL SURGING PERIODS FOR MARK 6 TYPE MINES
VERSUS CABLE LENGTH

Cable Length (Feet)	Natural Surging Period (Seconds)
100	20
300	35
500	45
1000	64
1500	79
2000	91

It is seen that the natural surge period is dominated by the cable length.¹⁰ It appears that resonance in the fundamental mode of surging would occur only

1. In very shallow mine plants exposed to long-period waves or a mixed sea in which long-period waves may be present.
2. In response to seiches, surf beat, or internal waves which normally have very long periods.

Since the natural period of the mine in surging is very large compared to normal wind-wave periods and the mine is virtually unrestrained in horizontal motion over short distances the mine case will follow the horizontal particle motion. This means that oscillatory flow forces due to horizontal particle motion will be very small and can be neglected where cable length exceeds about 100 feet.

SWAYING - Swaying motion can also be considered as practically unrestrained since the restoring force is identical to that in surging motion. Consequently, it can again be assumed that any transverse force on the mine case due to the horizontal particle motion associated with progressive waves can be neglected. Further, in the uniform, long-crested waves assumed in this study horizontal particle motion will produce forces in, or directly opposed to, the direction of wave motion. This means that exciting forces for mine swaying motion can originate only from eddies or from self excitation by the mine system. Since these forces are usually small mine swaying motion should be small compared to surging and consequently will be neglected herein.

¹⁰ The buoyancy and mass do not differ appreciably between mines of the same mark and mod.

3B4 OSCILLATORY FORCES ON A MINE CABLE

In what follows an attempt is made to examine the oscillatory flow forces on a mine cable. It will be recalled that in the discussion of deep-water waves it was shown that wave energy is concentrated close to the surface. This permits the neglect of wave forces on a cable in deep water. In shallow water, however, we have the opposite extreme, horizontal particle motion is for all practical purposes constant with depth. If it can be shown that cable forces are small in shallow water (they necessarily are even less in intermediate water) then it should be permissible to neglect cable forces in all depths. It will be noted that forces due to vertical particle motion have not been mentioned, the reason being that these are always less than the horizontal forces on a mine cable.¹¹ The case considered

will be that of a rigid, upright cable extending from the bottom to a point close to the surface as shown in Figure 13.

The horizontal force exerted on the differential section dz , at any instant, is the sum of the drag and the inertial forces.

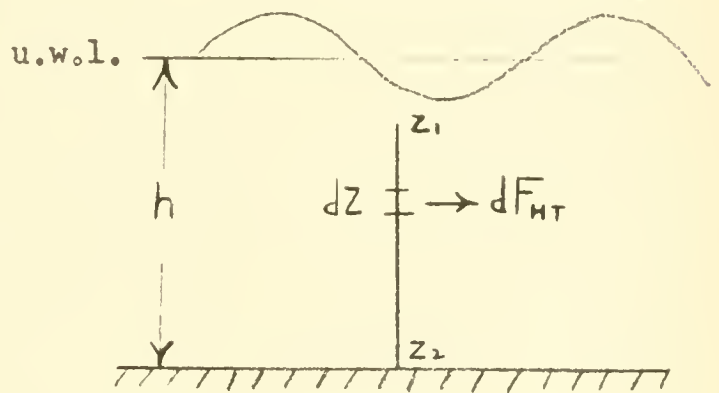


Figure 13 Forces on a Cable Segment due to Wave Motion.

$$dF_{HT} = \frac{1}{2} \int dC_D u^2 dz + \int C_M \left(\frac{\pi d^2}{4} \right) \frac{\partial u}{\partial t} dz$$

11 In deep and intermediate water at levels close to the surface, where vertical particle motion is appreciable, the cable inclination is small.

The total horizontal thrust on the cable at any instant is the sum of the drag and inertial forces integrated over the length of the cable.

$$F_{HT} = \int_{z_2}^{z_1} \frac{1}{2} d C_D u^2 dz + \int_{z_2}^{z_1} C_M \left(\frac{\pi d^2}{4} \right) \frac{\partial u}{\partial t} dz$$

If the horizontal particle velocity and acceleration for sine waves of small steepness u and $\frac{\partial u}{\partial t}$, respectively, are substituted in the foregoing equation there results

$$F_{HT} = \pm \int_{z_2}^{z_1} \frac{\pi^2 d}{2} C_D \frac{H^2}{T^2} \left[\frac{\cosh K(h+z)}{\sinh Kh} \right]^2 \cos^2 \theta dz + \int_{z_2}^{z_1} \frac{\pi^2 d^2}{2} C_M \frac{H}{T^2} \left[\frac{\cosh K(h+z)}{\sinh Kh} \right] \sin \theta dz$$

where $\theta = Kx - \sigma t$.

In shallow water

$$\frac{\cosh K(h+z)}{\sinh Kh} = \frac{1}{Kh}$$

$$C_s = \sqrt{gh}$$

$$L_s = \sqrt{gh} T$$

and the force equation reduces to

$$F_{HT} = \frac{\int H \sqrt{g} d}{8 \sqrt{h}} (z_1 - z_2) \left[\pm \frac{C_D H \sqrt{g}}{\sqrt{h}} \cos^2 \theta + \frac{2\pi^2 C_M d}{T} \sin \theta \right]$$

The double sign has been added to the drag term since it is no longer able to maintain a plus or minus sign by itself. The drag term takes the positive or negative sign depending on the sign of $\cos \theta$, i.e.,

$$\text{positive} \left\{ \begin{array}{l} 0 \leq \theta < \frac{\pi}{2} \\ \frac{3\pi}{2} < \theta \leq 2\pi \end{array} \right.$$

$$\text{negative} \quad \frac{\pi}{2} < \theta < \frac{3\pi}{2}$$

The inertial term is

$$\text{positive} \quad \pi < \theta < 2\pi$$

$$\text{negative} \quad 0 < \theta < \pi$$

which means the drag and inertial forces are in phase in the second and fourth quadrants.

The angular position ϕ where F_{HT} is a maximum is obtained by setting $\frac{\partial F_{HT}}{\partial \theta} = 0$ (ϕ is that value of θ where F_{HT} is a maximum).

The result is

$$\sin \phi = \frac{\pi^2 d C_M \sqrt{h}}{C_D TH \sqrt{g}} = 1.3 \frac{d \sqrt{h}}{TH}$$

Since the cable diameter d usually has a magnitude less than 0.04 and the denominator TH is always larger than \sqrt{h} when wave height is greater than one foot, $\sin \phi$ is a very small quantity. Thus, the maximum thrust occurs when θ is approximately 0° and 180° . This indicates that the inertial force is small compared to the drag force.

The maximum horizontal thrust is closely approximated by

$$F_{HT} = \pm \frac{C_D H^2 g d}{8h} (z_1 - z_2) = \frac{8C_D H^2 d}{h} (z_1 - z_2)$$

With a cable extending from the bottom to a point close to the sea surface, computations in Appendix G show maximum horizontal cable forces of approximately 50 lbs result from the passage of waves ten feet in height¹² in any water depth. The value of 50 lbs represents maximum expected thrust. In the actual case the cable would be inclined and free to move, which would lessen the wave force. The inclination of the cable acts in two ways to lessen the force. First, as in steady flow, when a cylinder is inclined the horizontal drag force is reduced.¹³ Second, the cable inclination means a change in phase of the wave force over different segments of the cable. In an extreme case the upper position of a cable might be experiencing a positive thrust due to a passing wave crest while the lower segment would be under a passing trough and feeling a thrust in the opposite direction. Thus, the forces would tend to cancel one another. Further, the calculations in Appendix G are based on the assumption that in shallow water horizontal particle motion is not attenuated with depth. Actually there is a little attenuation which would tend to decrease the actual force. Consequently, the oscillatory forces on the mine cable will be neglected hereafter. It should be remembered, however, that these forces, while small in magnitude, have a great bearing on the life expectancy of the cable. The continual flexing of the cable resulting from oscillatory flow leads to metal fatigue.

12 A wave ten feet in height would be considered higher than average for most locations.

13 See page 68, infra.

3B5 OSCILLATORY FORCES ON A SPHERICAL MINE CASE

It will be recalled in the discussion of mine motion it was concluded that the horizontal force on a mine case due to wave induced particle motion was small. Vertical forces on the mine case, however, can become appreciable under certain wave conditions. The aim in this section is to find the conditions, if any, under which oscillatory forces are operationally important. The problem considered will be that of a spherical mine case fixed in space as far as vertical motion is concerned.

The vertical force exerted on the mine case, at any instant, is the sum of the drag and inertial forces.

$$F_{VT} = \frac{1}{2} \int C_D \left(\frac{\pi}{4} d_M^2 \right) w^2 + \int C_M \left(\frac{\pi}{6} d_M^3 \right) \frac{\partial w}{\partial t}$$

If the vertical particle velocity and acceleration for waves of small steepness w and $\frac{\partial w}{\partial t}$, respectively, are substituted in the foregoing equation there results

$$F_{VT} = \pm \frac{1}{2} \int C_D \left(\frac{\pi}{4} d_M^2 \right) \frac{\pi^2 H^2}{T^2} \left[\frac{\sinh K(h+z)}{\sinh Kh} \right]^2 \sin^2 \theta - \int C_M \left(\frac{\pi}{6} d_M^3 \right) \frac{2\pi^2 H}{T^2} \left[\frac{\sinh K(h+z)}{\sinh Kh} \right] \cos \theta$$

where $\theta = Kx - \sigma t$ and the double sign has been added to the drag term to maintain the correct sign as discussed previously. The drag term takes the positive or negative sign depending on the sign of $-\sin \theta$, i.e.,

$$\text{positive} \quad \pi < \theta < 2\pi$$

$$\text{negative} \quad 0 < \theta < \pi$$

The inertial term is

$$\text{positive} \quad \frac{\pi}{2} < \theta < \frac{3\pi}{2}$$

$$\text{negative} \quad \left\{ \begin{array}{l} 0 \leq \theta < \frac{\pi}{2} \\ \frac{3\pi}{2} < \theta \leq 2\pi \end{array} \right.$$

which means the drag and inertial forces are in phase in the first and third quadrants.

If we set

$$\Lambda = \frac{\sinh K(h+z)}{\sinh Kh}$$

and rearrange a simplified force equation is obtained:

$$F_{VT} = \frac{\pi^2 d^2 \rho H \Lambda}{T^2} \left[+ \frac{C_H \Lambda}{8} \sin^2 \theta - \frac{d C_M}{3} \cos \theta \right]$$

The effect of varying wave characteristics, water depth, and mine case depth can be found by examining the foregoing force equation.

WAVE HEIGHT (H) - The total force increases as H increases but the drag force increases more rapidly than the inertial force.

WAVE PERIOD (T) - The total force decreases as T increases.

There is another secondary effect when T is increased; since the wave length is an increasing function of the period an increase in T increases the wave length, thus decreasing the value of Kh.

However, Kh decreases at a faster rate than K(h+z) and the factor $\frac{\sinh K(h+z)}{\sinh Kh}$ increases slowly. This in turn means total

force increases but the increase is negligible.

WATER DEPTH (h) - As water depth decreases the total force decreases because of the increasing restriction on vertical particle motion by the bottom boundary. The reduction in total force is given by the steadily decreasing factor $\frac{\sinh K(h+z)}{\sinh Kh}$.

The drag force decreases more rapidly than the inertial force since it is proportional to the square of the hyperbolic factor.¹⁴

In areas where tidal range is appreciable the resulting fluctuations in water depth periodically bring the mine case closer to the sea surface. This acts to increase the hyperbolic factor \wedge resulting in larger oscillatory forces.

MINE CASE DEPTH (z) - As the absolute value of the mine case depth z decreases, \wedge increases which increases the vertical oscillatory forces. Thus, larger forces are exerted on those mines moored close below the sea surface.

Summarizing the above discussion, it is evident that the following conditions lead to the greatest wave forces.

1. Steep waves (large H, small T).
2. Deep water.¹⁵
3. Mines moored close to the undisturbed level of the sea surface.

The angular position ϕ where F_{VT} is a maximum is obtained by

setting $\frac{\partial F_{VT}}{\partial \theta} = 0$ (ϕ is that value of θ where the maximum force occurs).

14 The hyperbolic factor \wedge is always less than unity.

15 It must be emphasized that the term deep water, as used herein, refers to the relative depth $\frac{h}{L}$. With respect to most ocean waves mines moored in water depths exceeding 100 feet are in deep water.

The result is

$$\cos \phi = - \frac{4d_M C_M}{3C_D H \Lambda} = - \frac{4d_M}{H \Lambda}$$

$$\sin^2 \phi = 1 - \frac{16d_M^2}{H^2 \Lambda^2} .$$

Λ is always less than unity for a mine case fixed below the surface; therefore, the absolute value of $\cos \phi$ is apparently greater than unity for all but very high waves. Since the absolute value of a cosine can not be greater than unity this means that $\phi = 180^\circ$ and the inertial term predominates. When waves become very high the influence of the drag component increases and the maximum force is a combination of inertial and drag components.

When $H \leq 12$ feet, the maximum vertical force consists of the inertial component alone

$$\begin{aligned} F_{VT} &= \frac{\pi^3 d_M^3}{3T^2} C_M \rho H \Lambda \\ &= 837 \frac{H \Lambda}{T^2} \end{aligned}$$

for a Mark 6 mine case.

Tables VI, VII, and VIII show values for the maximum calculated vertical forces exerted on a Mark 6 mine case moored at certain levels below the sea surface in the water depths shown. The values obtained confirm the conclusions reached earlier in this article, namely, that steep waves in deep water acting on mines moored close to the sea surface result in the greatest forces. Waves of this type are common in active storm areas.

The magnitude of the vertical oscillatory forces, while not sufficient to cause mine movement, make such movement more probable when the mine is exposed to a combination of current and waves. In effect, the oscillatory force periodically decreases the weight of the anchor.

TABLE VI

MAXIMUM VERTICAL WAVE FORCE EXERTED ON A MARK 6 MINE CASE
MOORED 20 FEET BELOW THE SEA SURFACE IN DEEP WATER

H (Feet)	Maximum F_{VT} (Lbs)			
	T = 6 (Sec.)	T = 8	T = 10	T = 12
6	71	53	39	29
8	94	71	52	39
10	118	89	65	49
12	142	107	78	59
15	177	134	98	73

TABLE VII

MAXIMUM VERTICAL WAVE FORCE EXERTED ON A MARK 6 MINE CASE
MOORED TEN FEET BELOW THE SEA SURFACE IN A
DEPTH OF 50 FEET (INTERMEDIATE DEPTH)

H (Feet)	Maximum F_{VT} (Lbs)		
	T = 6 (Sec.)	T = 8	T = 10
6	95	58	38
8	126	77	51
10	158	97	64
12	189	116	77
15	240	145	96

TABLE VIII

MAXIMUM VERTICAL WAVE FORCE EXERTED ON A MARK 6 MINE CASE
MOORED 20 FEET BELOW THE SEA SURFACE IN A
DEPTH OF 50 FEET (INTERMEDIATE DEPTH)

H (Feet)	Maximum F_{VT} (Lbs)		
	T = 6 (Sec.)	T = 8	T = 10
6	62	41	28
8	82	55	37
10	103	69	46
12	124	82	56
15	185	103	70

CHAPTER 4
CONCLUSIONS

Following are the major conclusions resulting from this study.

1. Mark 6 mines may move due to a combination of wave and steady flow forces. The wave forces periodically decrease the effective weight of the anchor enabling the current forces to drag or "walk" the anchor along the bottom.
2. Wave forces are maximum when waves are steep and the mine is moored close to the sea surface in water which is deep with respect to ocean waves. Most moored mine fields are located in water defined in this way as "deep".
3. Dip is the main problem in locations where only steady currents need be considered. Steady currents in excess of five knots are required to initiate movement of a Mark 6 anchor even on a smooth, hard bottom. Mark 6 mines would not be planted in areas where such strong currents exist.
4. Since the most important component of the wave force acts in the vertical direction and steady flow forces act in the horizontal direction a mine case shape to minimize movement and dip must meet conflicting requirements. Further, a mine case designed to produce a lift force when exposed to horizontal currents would be subject to strong vertical wave forces. The conflict may be resolved by designing a special mine case for use in rivers or protected waters and another mine case for use in open ocean areas. In the latter location it would appear, qualitatively, that a spherical mine case is optimum.

5. The increased drag due to marine growth is due primarily to increased cable diameter.¹

1 Debris or weedlike growths, such as kelp which may become entangled in the mine assemblage, were not considered in this study.

BIBLIOGRAPHY

1. Vennard, J. K. ELEMENTARY FLUID MECHANICS, 3rd Edition
John Wiley & Sons, 1954

2. Sverdrup, H. U., et.al. THE OCEANS
Prentice Hall, 1942

3. Kuenen, Ph. H. MARINE GEOLOGY
John Wiley & Sons, 1950

4. Schlichting, H. BOUNDARY LAYER THEORY
McGraw-Hill, 1955

5. Woods Hole Oceanographic MARINE FOULING AND ITS PREVENTION
Institution U. S. Naval Institute, 1952

6. Hoerner, S. AERODYNAMIC DRAG
Published by author, 1951

7. Young, A. D. THE DRAG EFFECTS OF ROUGHNESS AT HIGH
 SUBCRITICAL SPEEDS
Journal Royal Aeronautical Society,
Vol. 54, pp 534-540, 1950

8. Rouse, H. ELEMENTARY MECHANICS OF FLUIDS
John Wiley & Sons, 1946

9. Winney, H. F. VORTEX SYSTEM BEHIND A SPHERE MOVING
 THROUGH VISCOUS FLUID
Aero. Research Council (Great Britain)
Reports and Memoranda No. 1531

10. Relf, E. F. and THE FREQUENCY OF EDDIES GENERATED BY
 Simmons, L. F. G. THE MOTION OF CIRCULAR CYLINDERS
 THROUGH A FLUID
Aero. Research Council (Great Britain)
Reports and Memoranda No. 917

11. Delany, N. K. and LOW-SPEED DRAG OF CYLINDERS OF VARIOUS
 Sorensen, N. E. SHAPES
 NACA Technical Note 3038

12. Naval Ordnance Laboratory EXPERIMENTAL STUDIES OF DRAG
 NOLM 3024

13. Pode, L. TABLES FOR COMPUTING THE EQUILIBRIUM
 CONFIGURATION OF A FLEXIBLE CABLE IN A
 UNIFORM STREAM
David W. Taylor Model Basin Report 687

14. Eisenberg, P. CHARACTERISTICS OF THE NRL MARK 3 BOAT-TYPE BUOY AND DETERMINATION OF MOORING LINE SIZES
David W. Taylor Model Basin Report 550
15. Moritz, C. E. MINE WARFARE AND MARINE FOULING
Naval Ordnance Lab. Report 957
16. Wiegel, R. L. OSCILLATORY WAVES, SPECIAL ISSUE NO. 1
Beach Erosion Board, U. S. Army Corps of Engineers
17. Russell, R. C. H. and MacMillan, Commander D. H. WAVES AND TIDES
Philosophical Library, 1953
18. Hydrographic Office BREAKERS AND SURF PRINCIPLES IN FORECASTING
Hydrographic Office, U.S.N., H.O. 234
19. O'Brien, M. P. and Morison, J. R. THE FORCES EXERTED BY WAVES ON OBJECTS
Transactions, Amer. Geophysical Union, Vol. 33, pp 32-38, 1952
20. Morison, J. R., et.al. THE FORCE EXERTED BY SURFACE WAVES ON PILES
Journal Petroleum Tech., American Inst. Mining and Metal. Eng., Vol. 189, pp 149-154, 1950
21. Naval Ordnance Laboratory A STUDY OF MINE DIP
Naval Ordnance Lab Report 380
22. Iverson, H. W. and Balent, R. A CORRELATING MODULUS FOR FLUID RESISTANCE IN ACCELERATED MOTION
Journal of Applied Physics, Vol 22, pp 324-328, 1951
23. Lamb, H. HYDRODYNAMICS, 6th Edition
Dover Publications, 1945
24. United States Steel Corporation U. S. STEEL TIGER BRAND HANDBOOK FOR WESTERN WIRE ROPE USERS
U. S. Steel Corp., Columbia-Geneva Steel Division, 1956
25. Synge, J. A. and Griffith, B. A. PRINCIPLES OF MECHANICS
McGraw-Hill, 1942

APPENDIX A

CHAIN CHARACTERISTICS

Table IX contains approximate values for a few representative chain characteristics.

TABLE IX

WEIGHT AND SIZE CHARACTERISTICS OF UNCOATED
OR GALVANIZED STEEL PROOF COIL CHAINS

Trade Size ¹ (Inches)	Actual Size (Inches)	Over-all Width ² (Feet)	d_L Weight Per Foot (Lbs)	Weight Per Foot In Sea Water (Lbs)
3/16	7/32	6.8×10^{-2}	0.40	0.35
1/4	9/32	8.7×10^{-2}	0.70	0.61
5/16	11/32	10.7×10^{-2}	1.05	0.91
3/8	13/32	12.6×10^{-2}	1.58	1.37
1/2	17/32	16.5×10^{-2}	2.65	2.30

1 Trade size is 1/32 inch smaller than the actual diameter of the bar stock from which the chain is manufactured.

2 $d_L = 0.31 d_T$ for proof coil chains, where d_T is the actual size in inches [14].

APPENDIX B

WIRE ROPE ENGINEERING DATA

B1 STRETCH OF WIRE ROPES

The following are excerpts¹ from a United States Steel Corporation handbook [24] on wire rope.

The stretch of a wire rope under loads is the result of two components; the structural stretch, caused by lengthening of the rope lay, compression of the core, and adjustment of the wires and strands to the lead; and the elastic stretch caused by elongation of the wires.

The elastic stretch of a wire rope is directly proportional to the load and the length of rope under load, and inversely proportional to the metallic area and the modulus of elasticity. This applies only to loads which do not exceed the elastic limit of the rope. The elastic limit of a bright wire rope is approximately 55% of its breaking strength; and for galvanized ropes it is approximately 50%. The elastic stretch of a loaded wire rope can be determined by the formula:

$$S = \frac{T_e s}{A_w E}$$

where S = elastic stretch of the rope, in feet

T_e = tensile load on the rope, in lbs

s = length of the rope, in feet

A_w = metallic area of rope cross section in square inches

E = Modulus of Elasticity in lbs per square inch

For the wire ropes commonly used in mine moorings A_w is approximately

$$A_w = 0.4d^2$$

where d is the wire rope diameter in inches [24].

¹ A few minor notational changes have been made.

B2 MODULUS OF ELASTICITY

Quoting again from the same source:

The modulus of elasticity of a wire rope varies throughout its life and is dependent on the construction of the rope and the conditions under which it operates. This modulus increases during the useful life of the rope.

For a new wire rope of the type commonly used in mine moorings the modulus of elasticity is approximately

$$E = 12,000,000 \text{ lbs/sq. inch}$$

B3 WEIGHT AND STRENGTH CHARACTERISTICS

Table X contains approximate values for a few representative wire rope characteristics.

TABLE X
WIRE ROPE CHARACTERISTICS²

Diameter (d) (Inches)	Weight Per Foot (w') In Air (Lbs)	Weight Per Foot (w) In Sea Water (Lbs)	Metallic Area (A _w) of Rope Cross-Section (Sq. Inches)	Minimum Breaking Strength (Lbs)
1/4	0.10	0.09	0.025	5,090
5/16	0.16	0.14	0.039	7,900
3/8	0.23	0.20	0.056	11,100
7/16	0.31	0.27	0.076	14,700
1/2	0.40	0.35	0.10	19,000

² Weight and strength characteristics are from Knight's Modern Seaman-ship, 12th ed., D. Van Nostrand Co., Inc., values given are for 6 x 19 galvanized wire rope, high grade plow steel, fibre core.

It is to be emphasized that values given in this table apply only to wire rope of 6 x 19 construction. Usually wire of different construction is used for each mine cable size, e.g.,

6 x 24 construction is used for 7/16 inch diameter cables

6 x 19 construction is used for 5/16 inch diameter cables

1 x 37 construction is used for 1/4 inch diameter cable.

The difference in characteristics between 6 x 19 and 6 x 24 construction is small, but large differences may exist between 6 x 19 and 1 x 37 construction.

APPENDIX C

FORCES ON A MOORED MINE DUE TO UNIFORM FLUID FLOW

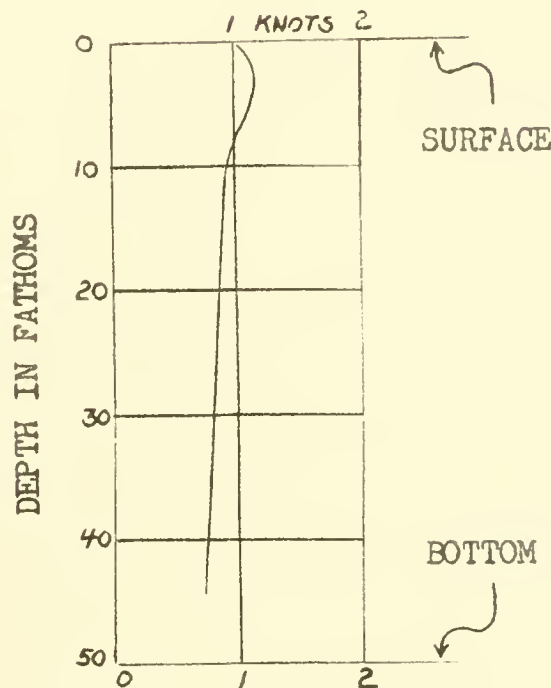
C1 GENERAL

There will be discussed below a method permitting the rapid calculation of the forces on a moored mine and mine dip due to steady current flow. The presentation closely follows that in NOLR 30 [21].

C2 ASSUMPTIONS

1. The sea surface and floor is horizontal and smooth.
2. The entire mooring is completely submerged.
3. The entire mooring lies in a vertical plane through the direction of motion. This assumption is not strictly valid even for a smooth cylinder in a uniform current because of the transverse hydrodynamic force due to the Von Karman vortex trail. With stranded cable an additional force normal to both the direction of flow and direction of cable element is introduced due to the asymmetric stranded profile. It is believed the error introduced by making this assumption is minor since the dip due to transverse forces on the cable are small compared to those in the direction of motion.
4. Current is uniform with depth. It is well known that current velocity usually decreases with depth, approaching zero at the bottom. In shallow water, however, up to about 50 fathoms deep, the current is often nearly constant except in the boundary layer close to the bottom. This is particularly true of tidal currents as shown in Figure 14.

The assumption of a uniform current compensates for the neglect of frictional drag on the cable and should give the maximum possible dip.



Factor for estimating
sub-surface rates

Figure 14 General Relation of Surface
to Sub-Surface Tidal Current.
(From Waves and Tides,
reference [17])

5. A specified cable section has a uniform weight in water per linear foot.
6. The cable is inextensible.
7. The mooring consists of a series of n wire cables and chains connected by flexible hinges. One end of the mooring is attached to the anchor, the other to the mine case with both connections also flexible. Assumed individual cable sections need not

terminate at a physical junction; the cable divisions are made to suit the problem under consideration.

8. The fluid drag on a section of cable inclined at an angle to the direction of flow can be resolved into components normal and tangential to the direction of the cable. If α_1 is the angle between the vertical and the cable section n_1 under consideration, then the force per unit length normal to the cable is given by $f_1 \cos^2 \alpha_1$ where f_1 is the force per unit length when the cable is normal to the flow.

The force per unit length parallel to the cable is given by a constant f_T for a given fluid velocity and in the ideal case will be due to frictional drag alone. If the cable is covered with marine growth this assumption is not valid. However, if we assume that an effective cable anti-fouling compound is used f_T can be neglected because of its small magnitude.¹

Neglect of f_T is incorrect when:

a. The cable is inclined at a large angle to the vertical over a considerable position of its length. Fortunately in a mine mooring the large angles occur close to the ocean floor where current is usually of reduced speed. Further, if large angles of inclination are encountered over a considerable length of the cable dip has already passed the critical stage.

1 See page 18, supra.

b. The cable is very long and f_T integrated over the length of the cable is an appreciable fraction of the forces at the ends of the cable.

C3 EQUATIONS OF MOORING

If the flexible cable section shown in Figure 15 is in equilibrium then equations describing its shape can be found by considering the normal and tangential components of the external forces acting upon the element of cable Δs .

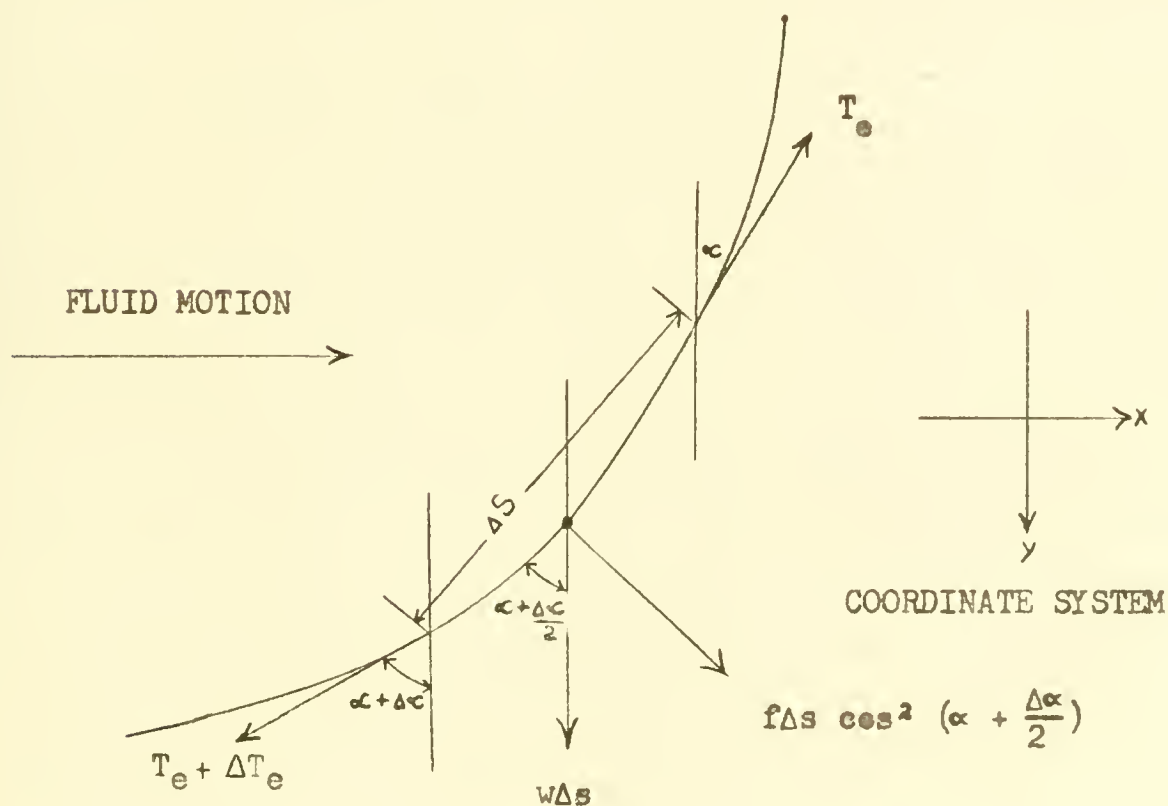


Figure 15 Forces on a cable segment.

NORMAL

$$f \Delta s \cos^2 \left(\alpha + \frac{\Delta \alpha}{2} \right) + w \Delta s \sin \left(\alpha + \frac{\Delta \alpha}{2} \right) - (T_e + \Delta T_e) \sin \frac{\Delta \alpha}{2} - T_e \sin \frac{\Delta \alpha}{2} = 0$$

Dividing by Δs

$$f \cos^2 \left(\alpha + \frac{\Delta \alpha}{2} \right) + w \sin \left(\alpha + \frac{\Delta \alpha}{2} \right) - \frac{(T_e + \Delta T_e)}{\Delta s} \sin \frac{\Delta \alpha}{2} - \frac{T_e}{\Delta s} \sin \frac{\Delta \alpha}{2} = 0$$

$$\sin \frac{\Delta \alpha}{2} \doteq \frac{\Delta \alpha}{2}$$

$$f \cos^2 \left(\alpha + \frac{\Delta \alpha}{2} \right) + w \sin \left(\alpha + \frac{\Delta \alpha}{2} \right) - \frac{(T_e + \Delta T_e) \Delta \alpha}{2 \Delta s} - \frac{T_e \Delta \alpha}{2 \Delta s} = 0$$

Allowing $\Delta \alpha$ and Δs to approach zero and neglecting the second order term

$$f \cos^2 \alpha + w \sin \alpha - \frac{T_e}{2} \frac{d\alpha}{ds} - \frac{T_e}{2} \frac{d\alpha}{ds} = 0$$

$$f \cos^2 \alpha + w \sin \alpha = T_e \frac{d\alpha}{ds} \quad (1)$$

TANGENTIAL

$$w \Delta s \cos \left(\alpha + \frac{\Delta \alpha}{2} \right) + T_e \cos \frac{\Delta \alpha}{2} - (T_e + \Delta T_e) \cos \frac{\Delta \alpha}{2} = 0$$

Dividing by Δs

$$w \cos \left(\alpha + \frac{\Delta \alpha}{2} \right) + \frac{T_e}{\Delta s} \cos \frac{\Delta \alpha}{2} - \frac{(T_e + \Delta T_e)}{\Delta s} \cos \frac{\Delta \alpha}{2} = 0$$

Allow $\Delta \alpha$ and Δs to approach zero

$$w \cos \alpha = \frac{dT_e}{ds} \quad (2)$$

An additional equation obtained by a consideration of the differential triangle in Figure 16 is

$$\frac{dy}{ds} = \cos \alpha \quad (3)$$

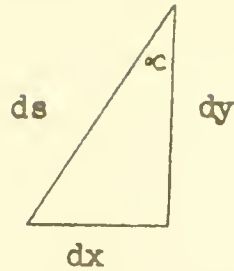


Figure 16 Differential Triangle.

Equations (1), (2), and (3) may be combined and a solution obtained by numerical or graphical integration. This method, though very accurate, is tedious. A simpler method is explained below which is nearly as accurate. A high degree of mathematical accuracy does not contribute to the precision of the final solution since the uniform oceanographic conditions assumed are only approximated.

C4 STRAIGHT LINE METHOD

If we make the additional assumption that each of the n sections in the mooring is stiff and straight we can then treat each section as a rigid body, obtain the dip due to the forces acting on the section, then sum over all such sections for the total dip.

Derivation

Consider a free body diagram of cable section C_1 shown in Figure 17.

Summation horizontal forces

$$X_1 + F_1 \cos^3 \alpha_1 - X'_1 = 0$$

$$X'_1 = X_1 + F_1 \cos^3 \alpha_1 \quad (4)$$

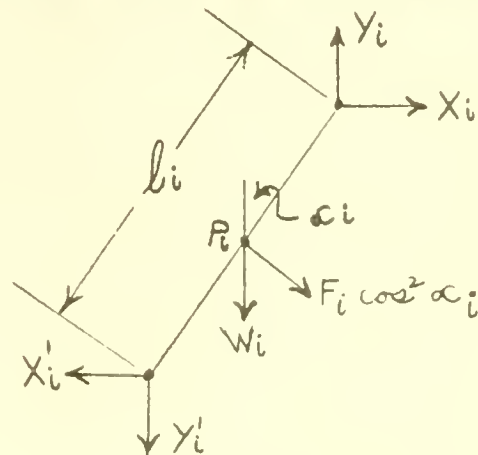


Figure 17 Free body diagram of a cable segment.

Summation vertical forces

$$Y_1 - W_1 - F_1 \cos^2 \alpha_1 \sin \alpha_1 - Y_1' = 0$$

$$Y_1' = Y_1 - W_1 - F_1 \cos^2 \alpha_1 \sin \alpha_1 . \quad (5)$$

Taking moments about the midpoint

$$Y_1' + Y_1 \frac{l_1}{2} \sin \alpha_1 = X_1' + X_1 \frac{l_1}{2} \cos \alpha_1$$

$$(Y_1' + Y_1) \sin \alpha_1 = (X_1' + X_1) \cos \alpha_1 . \quad (6)$$

Equations (4), (5), and (6) may be combined to obtain

$$\tan \alpha_1 = \frac{2X_1 + F_1 \cos \alpha_1}{2Y_1 - W_1} . \quad (7)$$

We now have an equation in which α_1 is the only unknown. To find the value of α_1 the method of successive approximations is used, i.e., estimate a value for α_1 , call this estimate β_1 , substitute in (7) to find

$$\tan \beta_1 = \frac{2X_1 + F_1 \cos \beta_1}{2Y_1 - W_1} = G_1 .$$

If this is not an equality repeat the process using a new estimate of α_1 called γ_1 . For the estimate on γ_1 it will be found that choosing $\gamma_1 = \arctan G_1$ will generally bring about convergence (to degree of accuracy desired) and no further approximations need be made. With experience β_1 can be estimated very closely from the known drag and buoyant forces.

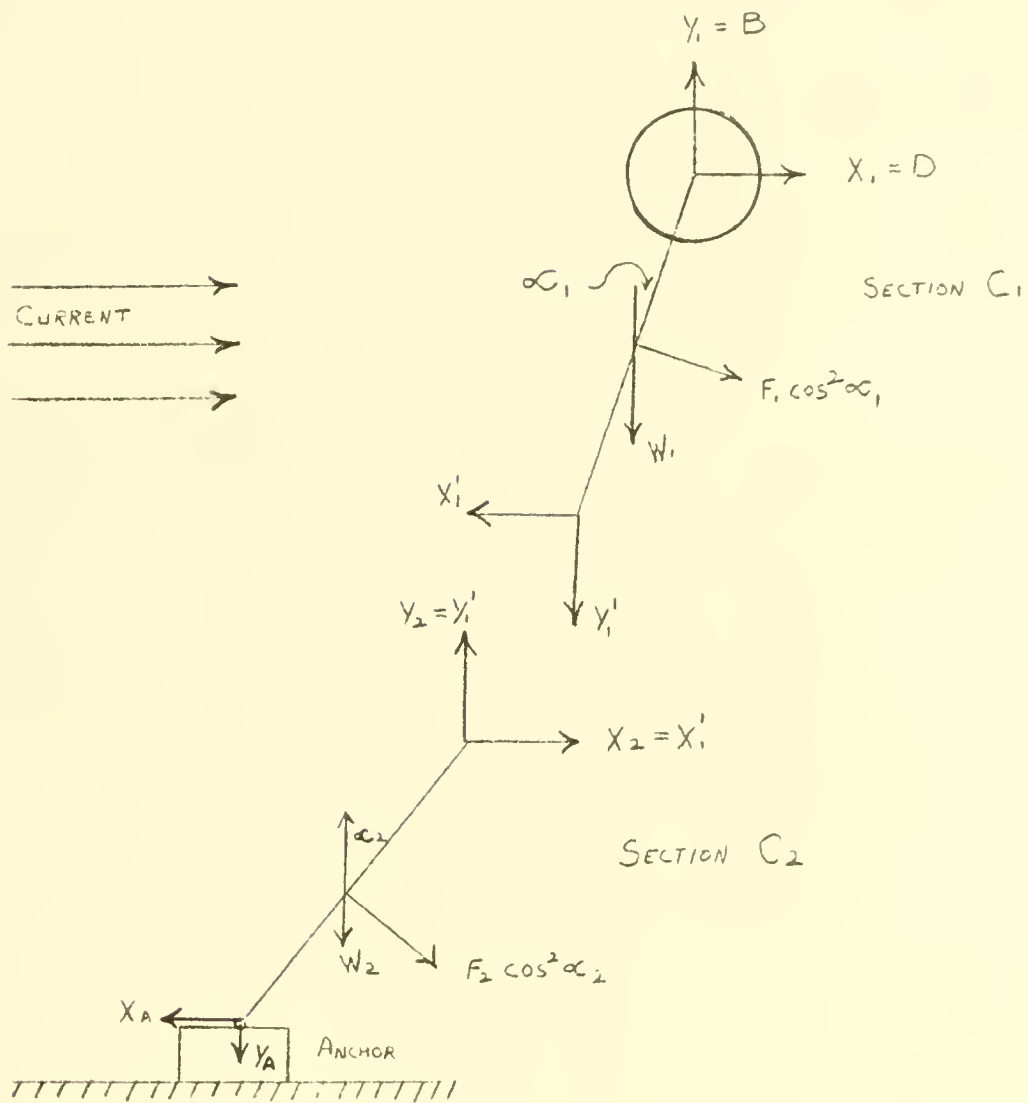


Figure 18 Forces on a Moored Mine and Cable.

For the succeeding section C_j equilibrium considerations require that $X_j = X_1'$ and $Y_j = Y_1'$; see Figure 18. X_j and Y_j may then be found using equations (4) and (5).

$$X_j = X_1' = X_1 + F_1 \cos^3 \alpha_1$$

$$Y_j = Y_1' = Y_1 - W_1 - F_1 \cos^2 \alpha_1 \sin \alpha_1$$

The angle α_j is now calculated in exactly the same way and the process is repeated over all cable sections.

To find the dip δ_1 consider the section C_1 in Figure 19.

$$\delta_1 + l_1 \cos \alpha_1 = l_1$$

$$\delta_1 = l_1 (1 - \cos \alpha_1)$$

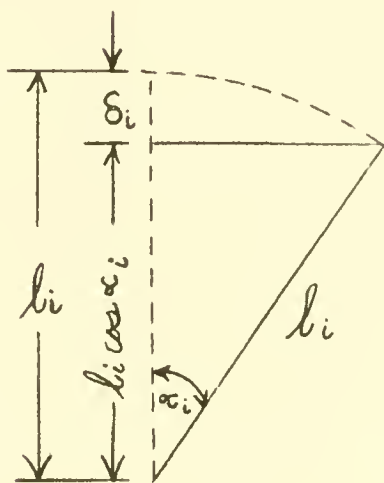


Figure 19 Cable Segment.

The total dip δ_T is then found by summing the individual δ_1 's.

$$\delta_T = l_1 (1 - \cos \alpha_1) + l_2 (1 - \cos \alpha_2) + \dots + l_i (1 - \cos \alpha_i) + \dots + l_n (1 - \cos \alpha_n) \quad (8)$$

With a homogeneous mooring, calculations are simplified by choosing sections of uniform length, $l_1 = l_2 = l_3 = \dots l_n$.

Then

$$F_1 = F_2 = F_3 = \dots F_i = F_j = \dots F_n$$

$$W_1 = W_2 = W_3 = \dots W_i = W_j = \dots W_n$$

and

$$\delta_T = l \left[(1 - \cos \alpha_1) + (1 - \cos \alpha_2) + \dots (1 - \cos \alpha_i) + \dots (1 - \cos \alpha_n) \right]$$

If for any reason it is not possible or convenient to choose all sections of uniform length it will simplify calculations if $n - 1$ equal sections and 1 odd section is used.

The choice of l is governed by the degree of curvature of the cable. NOLR 380 [21] states that for one percent accuracy l should be chosen so that the increase of α from one section to the next is less than 15° . Since the curvature of the cable depends on drag forces, cable weight, and mine buoyancy, the section lengths to be used can be easily estimated with a little experience.

For wire rope mooring cables less than 1/2 inch in diameter exposed to currents less than two knots, 100 foot sections usually give good results. With increasing currents, chain moorings, and shallow water, shorter section lengths are required.

C5 NUMERICAL EXAMPLES

1. A Mark 6 mine with

$$A_M = 7.03 \text{ ft}^2 \text{ (Based on case diameter of } 35 \frac{13}{16} \text{ inches)}$$

$$B = 278 \text{ lbs}$$

$$C_D = 0.5$$

is moored below the sea surface with 73 feet of 7/16-inch diameter wire cable having²

$$C_D = 2.00$$

$$w = 0.27 \text{ lbs/ft}$$

$$d = 0.0364 \text{ feet}$$

in a location where a uniform three knot (5.07 ft/sec.) current is running. What dip may be expected?

The drag force on the mine case is

$$D = \frac{1}{2} C_D \rho A_M U^2 = \frac{1}{2} (0.5)(2)(7.03)(5.07)^2 = 90.6 \text{ lbs}$$

The cable drag force is

$$f = \frac{1}{2} C_D \rho A U^2 = \frac{1}{2} (2)(2)(3.64 \times 10^{-2})(5.07)^2 = 1.88 \text{ lbs/ft}$$

While this problem may be solved using only two cable sections, in order to fully demonstrate the method involved we will divide the cable into one 13 foot section and five 12 foot sections with the 13 foot section = C₁ (attached to mine).

$$W_1 = w l_1 = 0.27(13) = 3.5 \text{ lbs}$$

$$W_{2,3,\dots,6} = w (l_{2,3,\dots,6}) = 0.27 (12) = 3.2 \text{ lbs}$$

$$F_1 = f l_1 = 1.88 (13) = 24.6 \text{ lbs}$$

$$F_{2,3,\dots,6} = f (l_{2,3,\dots,6}) = 1.88 (12) = 22.6 \text{ lbs}$$

$$X_1 = D = 90.6 \text{ lbs}$$

$$Y_1 = B = 278 \text{ lbs}$$

2 Since the same cable is used throughout the mooring no subscripts are necessary on C_D, w, or f.

$$\text{From (7) } \tan \alpha_1 = \frac{2X_1 + F_1 \cos \alpha_1}{2Y_1 - W}$$

For a first estimate choose $\beta_1 = 19.8^\circ$. This choice was made after the following reasoning:

$$\text{Arctan } \beta_1 = \frac{X_1}{Y_1} = \frac{90.6}{278}, \text{ but we guess the angle } \beta_1 \text{ will be}$$

increased due to cable drag and arbitrarily say

$$\text{arctan } \beta_1 = \frac{100}{278} = 3.6.$$

Therefore, $\beta_1 = 19.8^\circ$.

Using this approximation

$$\begin{aligned} \tan \beta_1 &= \frac{2X_1 + F_1 \cos \beta_1}{2Y_1 - W_1} \\ &= \frac{181.2 + 24.6 (0.94)}{556 - 3.5} = 0.37 \end{aligned}$$

$$\text{Arctan } 0.37 = 20.3^\circ$$

This differs from 19.8° by only 0.5° and α_1 could be safely assumed to be 20.3° since the expression $2X_1 + F_1 \cos \beta_1$ is relatively insensitive to small changes in β . However, in order to demonstrate the method a fairly exact solution will be obtained.

For the second approximation use $\gamma_1 = 20.3^\circ$.

Then

$$\tan \gamma_1 = \frac{181.2 + 24.6 (0.94)}{552.5} = 0.37.$$

Since we have agreement, call $\alpha_1 = 20.3^\circ$.

Proceeding to the second section C_2 ,

$$X_2 = X_1 + F_1 \cos^3 \alpha_1 = 90.6 + 24.6 (0.82) = 110.8 \text{ lbs}$$

$$Y_2 = Y_1 - W_1 - F_1 \cos^2 \alpha_1 = 278 - 3.5 - 24.6 (0.88)(0.35) = 267 \text{ lbs}$$

Estimate $\beta_2 = 29^\circ$.

$$\tan \beta_2 = \frac{2X_2 + F_2 \cos \beta^2}{2Y_2 - W_2} = \frac{221.6 + 22.6 (0.88)}{534 - 3.2}$$

$$= 0.455$$

$$\text{Arctan } 0.455 = 24.5^\circ$$

Estimate $\gamma_2 = 24.5^\circ$.

$$\tan \gamma_2 = \frac{221.6 + 22.6 (.91)}{530.8} = \frac{242.2}{530.8} = 0.456$$

Since we have agreement, call $\alpha_2 = 24.5^\circ$.

The process is repeated over the remaining four sections, obtaining

$$\alpha_3 = 28.5^\circ$$

$$\alpha_4 = 32.2^\circ$$

$$\alpha_5 = 35.8^\circ$$

$$\alpha_6 = 39^\circ$$

From (7) dip is

$$\begin{aligned} \delta_T &= l_1 (1 - \cos \alpha_1) + l_{2,3,\dots,6} [(1 - \cos \alpha_2) + (1 - \cos \alpha_3) + \dots + (1 - \cos \alpha_6)] \\ &= 13 (1 - 0.94) + 12 [(1 - 0.91) + (1 - 0.88) + (1 - 0.85) + (1 - 0.81) + (1 - 0.78)] \\ &= 10.1 \text{ feet} \end{aligned}$$

A Mark 6 mine under the stated conditions can then be expected to be about ten feet below set depth.

Table XI compares dip values obtained in this problem, using different section combinations.

TABLE XI

COMPARISON OF DIP VALUES OBTAINED USING VARIOUS SECTION COMBINATIONS

<u>Number of Cable Sections</u>	<u>Length of Each Section</u>	<u>Section Inclination</u>	<u>Maximum Change in Angle of Inclination Between Sections</u>	<u>Total Dip</u>
6	$l_1 = 13$	$\alpha_1 = 20.3$	4	10.1
	$l_{2,3,\dots,6} = 12$	$\alpha_2 = 24.5$		
		$\alpha_3 = 28.5$		
		$\alpha_4 = 32.2$		
		$\alpha_5 = 35.8$		
		$\alpha_6 = 39$		
3	$l_1 = 25$	$\alpha_1 = 22.3$	7.8	10.1
	$l_2 = 24$	$\alpha_2 = 30.1$		
	$l_3 = 24$	$\alpha_3 = 37.2$		
2	$l_1 = 36$	$\alpha_1 = 23.9$	11.3	10.0
	$l_2 = 37$	$\alpha_2 = 35.2$		
1	$l = 73$	$\alpha = 29.2$		9.3

It is to be noted that little difference exists in the dip whether the cable is divided into two, three, or six sections. This is to be

expected since the change in angle of inclination does not exceed 15 degrees in any case. The table also shows that little is to be gained by dividing the cable into more sections than necessary.

2. A Mark 6 mine case with

$$A_M = 7.03 \text{ ft}^2$$

$$B = 278 \text{ lbs}$$

$$C_D = 0.5$$

is moored below the sea surface with 100 feet of 7/16-inch diameter wire cable having

$$C_D = 2.0$$

$$w = 0.27 \text{ lbs/ft}$$

$$d = 0.0364 \text{ feet}$$

in a location where a uniform three knot (5.07 ft/sec.) current is running.

(a) What dip may be expected?

The drag force on the mine case, $D = 90.6 \text{ lbs}$, and the cable drag force per unit length, $f = 1.88 \text{ lbs/ft}$, from example number one.

Dividing the cable into two 50 foot sections, we have,

$$w = w\ell = 0.27 (50) = 13.5 \text{ lbs}$$

$$f = f\ell = 1.88 (50) = 94 \text{ lbs.}$$

For the first section C_1 ,

$$X_1 = D = 90.6 \text{ lbs}$$

$$Y_1 = B = 278 \text{ lbs}$$

Estimate $\beta_1 = 26^\circ$

$$\tan \beta_1 = \frac{181.2 + 84.5}{556 - 13.5} = 0.49$$

Call $\alpha_1 = 26.1^\circ$

For the second section C_2

$$X_2 = X_1 + F_1 \cos^3 \alpha_1 = 90.6 + 94 (0.72) = 158.2 \text{ lbs}$$

$$\begin{aligned} Y_2 &= Y_1 - W_1 - F_1 \cos^2 \alpha_1 \sin \alpha_1 \\ &= 278 - 13.5 - 94 (.81)(.44) = 231 \text{ lbs} \end{aligned}$$

Estimate $\beta_2 = 41^\circ$

$$\tan \beta_2 = \frac{316.4 + 71}{462 - 13.5} = 0.865$$

Call $\alpha_2 = 40.8^\circ$

From (7) dip is

$$\begin{aligned} \delta_T &= 50 \left[(1 - \cos 26.1^\circ) + (1 - \cos 40.8^\circ) \right] \\ &= 17.3 \text{ feet} \end{aligned}$$

(b) What are the forces transmitted to the anchor?

Consider Figure 18

$$\begin{aligned} X_A &= X_2 + F_2 \cos^3 \alpha_2 \\ &= 158.2 + 94 (.41) = 197 \text{ lbs} \\ Y_A &= Y_2 - W_2 - F_2 \cos^2 \alpha_2 \sin \alpha_2 \\ &= 231 - 13.5 - 94 (.56)(.65) = 183.3 \text{ lbs} \end{aligned}$$

APPENDIX D

OVERTURNING MOMENT ON A MARK 6 ANCHOR

Consider Figure 20 which shows a Mark 6 anchor subjected to a slowly increasing force F_A , such as might occur with an increasing tidal current.

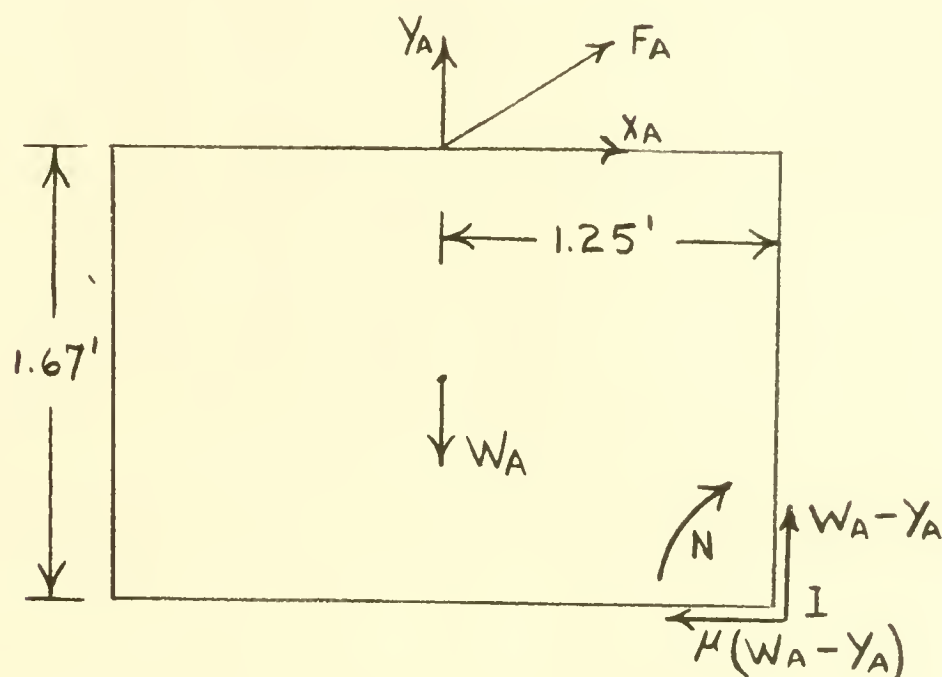


Figure 20 External Forces acting on a Mark 6 Anchor

Assume:

1. Anchor rests on a flat bottom.
2. Sea surface is smooth.
3. Anchor does not dig in at point 1, nor is its movement restricted by some irregularity about which it may pivot.
4. As F_A slowly increases, X_A increases but Y_A decreases.
5. Weight of the anchor W_A acts through the geometric center of the anchor.

Then, from Mechanics [25] ,

if $X_A \leq \mu (W_A - Y_A)$ sliding will not occur;

if $X_A \leq \frac{1.25}{1.67} (W_A - Y_A)$ the anchor will not overturn.

Thus, when $\mu \leq \frac{1.25}{1.67}$ the mine will begin to slide rather than overturn.

Conversely, if $\mu \geq \frac{1.25}{1.67}$ the mine will overturn before it begins to slide.

In order to find the magnitude of the forces necessary to cause overturning, take moments about point 1 .

$$\begin{aligned} N &= 1.67(X_A) + 1.25(Y_A) - 1.25(W_A) \\ &= 1.67 X_A - 1.25(W_A - Y_A) \end{aligned}$$

At the instant when $X_A = 0.75(W_A - Y_A)$, $N = 0$, and any further increase in X_A may cause overturning.

The current changes resulting in an increasing X_A necessarily decrease Y_A from its zero current value (about 150 lbs for a Mark 6 mine moored with 500 feet of 7/16 inch wire rope). Thus, for an anchor with $W_A = 786$ lbs, horizontal forces on the anchor exceeding about 600 lbs are required for overturning. Horizontal anchor forces of this magnitude are very unlikely.

APPENDIX E

NATURAL HEAVING PERIOD OF A MARK 6 MINE

If the mine case¹ has a diameter of three feet, weighs 495 lbs, and is moored with 500 feet of 7/16 inch diameter wire rope cable having

$$A_w = 0.0765 \text{ in.}^2$$

$$E = 12 \times 10^6 \text{ lbs/in.}^2$$

$$w' = 0.31 \text{ lbs/ft}$$

then

$$M = \frac{W_M}{g} = \frac{495}{32.2} = 15.4 \text{ slugs}$$

$$qM^* = q \int V = 0.5(2)(14.1) = 14.1 \text{ slugs}$$

$$M_c = \frac{1}{3} \frac{w' S}{g} = \frac{(0.31)(500)}{(3)(32.2)} = 1.6 \text{ slugs}$$

$$M_e = M + qM^* + M_c = 31.2 \text{ slugs}$$

$$T_e = 2\pi \sqrt{\frac{SM_e}{EA_w}} = 0.8 \text{ sec.}$$

1 The volume V of the mine case has been calculated as though the mine were a perfect sphere. Protrusions and indentations have been neglected.

APPENDIX F

NATURAL SURGING PERIOD OF A MARK 6 MINE

If the mine case¹ has the following characteristics

$$d_M = 3 \text{ feet}$$

$$B = 283 \text{ lbs}$$

$$W_M = 495 \text{ lbs}$$

$$V = 14.1 \text{ cu. ft}$$

and is moored with 500 feet of cable, then

$$M = \frac{495}{32.2} = 15.4 \text{ slugs}$$

$$qM = q \int V = 0.5(2)(14.1) = 14.1 \text{ slugs}$$

$$S = 500 \text{ feet}$$

$$T = \frac{2\pi}{\sqrt{\frac{B}{S(M+qM)}}} = 45 \text{ sec.}$$

1 The volume V of the mine case has been calculated as though the mine were a perfect sphere. Protrusions and indentations have been neglected.

APPENDIX G

MAXIMUM HORIZONTAL WAVE FORCE
EXERTED ON MINE CABLES IN SHALLOW WATER

The classification, shallow water, requires that $\frac{h}{L_0} < \frac{1}{25}$. To meet this requirement the wave periods and deep water length must be large, as shown in Table XIII.

TABLE XIII

THE DEEP WATER LENGTHS AND PERIODS
OF SHALLOW WATER WAVES IN CERTAIN DEPTHS

<u>Depth h</u> <u>(Feet)</u>	<u>Deep Water Wave Length L_0</u> <u>(Feet)</u>	<u>Period T</u> <u>(Seconds)</u>
50	1250	15.6
100	2500	22.2

Example 1.

Assume a rigid upright mine cable 7/16 inches in diameter, extending from the bottom to a point ten feet from the sea surface. If the water depth is 50 feet compute the maximum thrust on the cable resulting from the passage of a wave having a height of ten feet and a period of 15.6 seconds.

From article 3B4

$$\overline{F}_{HT} = \frac{8C_D H^2 d}{h} (z_1 - z_2)$$

$$\overline{F_{HT}} = + \frac{8(2)(100)(0.0364)(40)}{50}$$

$$\left| \overline{F_{HT}} \right| = 47 \text{ lbs}^1$$

Example 2.

Repeat the foregoing calculation for a water depth of 100 feet and a wave period of 22.1 seconds.

$$\overline{F_{HT}} = + \frac{8(2)(100)(0.0364)(90)}{100}$$

$$\left| \overline{F_{HT}} \right| = 52 \text{ lbs}^1$$

1 The values calculated here are somewhat large since in the actual case the cable is inclined and free to move. See page 51, supra.

APPENDIX H

MAXIMUM VERTICAL WAVE FORCE EXERTED ON A MINE CASE

Example 1.

The first example will consider a Mark 6 mine moored in an intermediate water depth (with respect to ocean waves) and subjected to waves less than 12 feet in height. Assume:

$$h = 50 \text{ feet}$$

$$z = - 10 \text{ feet}$$

$$d_M = 3 \text{ feet}$$

$$C_M = 1.5$$

$$C_D = 0.5$$

$$\rho = 2 \text{ slugs/ft}^3$$

$$T = 10 \text{ seconds}$$

$$H = 10 \text{ feet}$$

Calculations:

From article 3A2

$$L_o = 5.12T^2 = 512 \text{ feet}$$

$$\frac{h}{L_o} = \frac{50}{512} = 0.0977$$

From¹ Figure 9

$$\frac{h}{L} = 0.139, \therefore L = 360 \text{ feet}$$

¹ This value may be obtained from Special Issue No. 1, Beach Erosion Board [16] with greater accuracy than permitted by Figure 9.

The following equations are obtained from article 3B5

$$\Lambda = \frac{\sinh K(h+z)}{\sinh K} = \frac{\sinh \frac{2\pi(50-10)}{360}}{\sinh \frac{2\pi(50)}{360}} = 0.765$$

For a Mark 6 mine when $H \leq 12$ feet

$$F_{VT} = 837 \frac{H\Lambda}{T^2} = \frac{837(10)(0.765)}{100} = 64 \text{ lbs}$$

Example 2.

Consider a Mark 6 mine moored in deep water (with respect to ocean waves) subjected to waves greater than 12 feet in height. Assume:

$$h = 500 \text{ feet}$$

$$z = -20 \text{ feet}$$

$$d_M = 3 \text{ feet}$$

$$C_M = 1.5$$

$$C_D = 0.5$$

$$\rho = 2 \text{ slugs/ft}^3$$

$$T = 10 \text{ seconds}$$

$$H = 20 \text{ feet}$$

Calculations:

$$\text{In deep water } L = 5.12T^2 = 512 \text{ feet.}$$

The following equations are obtained from article 3B5:

$$\Lambda = \frac{\sinh K(h+z)}{\sinh Kh}$$

For the special case of a mine moored close to the sea surface in deep water this equation can be simplified to:

$$\Lambda = e^{-Kz}$$

$$\Lambda = e^{-\frac{2\pi(20)}{512}} = 0.783$$

The angular position of maximum vertical force is

$$\cos \phi = -\frac{4d_M C_M}{3C_D H \Lambda} = -0.77$$

$$\phi = 140^\circ 21'$$

$$\sin \phi = 0.64$$

The general equation for the vertical force is

$$F_{VT} = \frac{\pi^3 d_M^2 H \Lambda}{T^2} \left[\pm \frac{C_D H \Lambda}{8} (\sin^2 \theta) - \frac{d_M C_M}{3} \cos \theta \right]$$

where the plus or minus is chosen as the $-\sin \theta$ and therefore will be positive in this example.

$$F_{VT} = \frac{\pi^3 (9)(2)(20)(0.783)}{100} \left[\frac{(0.5)(20)(0.783)}{8} (0.41) - \frac{(3)(1.5)(0.77)}{3} \right] = 169 \text{ lbs.}$$

$$\Lambda = e^{-\frac{2\pi(20)}{512}} = 0.783$$

The angular position of maximum vertical force is

$$\cos \phi = -\frac{4d_M C_M}{3C_D H \Lambda} = -0.77$$

$$\phi = 140^\circ 21'$$

$$\sin \phi = 0.64$$

The general equation for the vertical force is

$$F_{VT} = \frac{\pi^3 d_M^2 H \Lambda}{T^2} \left[\pm \frac{C_D H \Lambda}{8} (\sin^2 \theta) - \frac{d_M C_M}{3} \cos \theta \right]$$

where the plus or minus is chosen as the $-\sin \theta$ and therefore will be positive in this example.

$$F_{VT} = \frac{\pi^3 (9)(2)(20)(0.783)}{100} \left[\frac{(0.5)(20)(0.783)}{8} (0.41) - \frac{(3)(1.5)(0.77)}{3} \right] = 169 \text{ lbs.}$$

thesM252

Steady and oscillatory flow forces on a



3 2768 001 88263 2

DUDLEY KNOX LIBRARY